



HAL
open science

Genetic analysis of praziquantel response in schistosome parasites implicates a Transient Receptor Potential channel

Winka Le Clec'h, Frédéric D Chevalier, Ana Carolina A Mattos, Amanda Strickland, Robbie Diaz, Marina Mcdew-White, Claudia M Rohr, Safari Kinung'hi, Fiona Allan, Bonnie L Webster, et al.

► To cite this version:

Winka Le Clec'h, Frédéric D Chevalier, Ana Carolina A Mattos, Amanda Strickland, Robbie Diaz, et al.. Genetic analysis of praziquantel response in schistosome parasites implicates a Transient Receptor Potential channel. *Science Translational Medicine*, 2021, 13 (625), pp.eabj9114. 10.1126/scitranslmed.abj9114 . hal-03428154

HAL Id: hal-03428154

<https://hal.science/hal-03428154>

Submitted on 15 Nov 2021

HAL is a multi-disciplinary open access archive for the deposit and dissemination of scientific research documents, whether they are published or not. The documents may come from teaching and research institutions in France or abroad, or from public or private research centers.

L'archive ouverte pluridisciplinaire **HAL**, est destinée au dépôt et à la diffusion de documents scientifiques de niveau recherche, publiés ou non, émanant des établissements d'enseignement et de recherche français ou étrangers, des laboratoires publics ou privés.

1 **Genetic analysis of praziquantel resistance in schistosome parasites implicates a Transient Receptor**
2 **Potential channel**

3

4 Winka Le Clec'h^{1*§}, Frédéric D. Chevalier^{1§}, Ana Carolina A. Mattos², Amanda Strickland¹, Robbie Diaz¹,
5 Marina McDew-White¹, Claudia M. Rohr³, Safari Kinung'hi⁴, Fiona Allan^{5,6}, Bonnie L Webster^{5,6}, Joanne
6 P Webster^{5,7}, Aidan M Emery^{5,6}, David Rollinson^{5,6}, Amadou Garba Djirmay^{8,9}, Khalid M Al Mashikhi
7 ¹⁰, Salem Al Yafae¹⁰, Mohamed A Idris¹¹, Hélène Moné¹², Gabriel Mouahid¹², Philip LoVerde², Jonathan
8 S. Marchant³, Timothy J.C. Anderson^{1*}

9

10 ¹ Texas Biomedical Research Institute; San Antonio, TX

11 ² University of Texas Health Science Center at San Antonio; San Antonio, TX 78229

12 ³ Department of Cell Biology, Neurobiology and Anatomy, Medical College of Wisconsin;

13 Milwaukee WI 53226, USA.

14 ⁴ National Institute for Medical Research, Mwanza, United Republic of Tanzania

15 ⁵ London Centre for Neglected Tropical Disease Research (LCNDTR), Imperial College, London, United
16 Kingdom

17 ⁶ Wolfson Wellcome Biomedical Laboratories, Natural History Museum, London, United Kingdom

18 ⁷ Centre for Emerging, Endemic and Exotic Diseases (CEEED), Royal Veterinary College, University of
19 London, United Kingdom

20 ⁸ Réseau International Schistosomiases Environnemental Aménagement et Lutte (RISEAL), Niamey, Niger

21 ⁹ World Health Organization, Geneva, Switzerland

22 ¹⁰ Directorate General of Health Services, Dhofar Governorate, Salalah, Sultanate of Oman

23 ¹¹ Sultan Qaboos University, Muscat, Sultanate of Oman

24 ¹² Host-Pathogen-Environment Interactions laboratory, University of Perpignan, Perpignan, France

25 [§] These authors contributed equally to this work.

26 ^{*}Correspondence to: winkal@txbiomed.org (WL), tanderso@txbiomed.org (TA)

27 **One Sentence Summary:** A transient receptor potential channel determines variation in praziquantel-
28 response in *Schistosoma mansoni*.
29

30 **Abstract:**

31 Mass treatment with praziquantel (PZQ) monotherapy is the mainstay for schistosome treatment. This drug
32 shows imperfect cure rates in the field and parasites showing reduced response to PZQ can be selected in
33 the laboratory, but the extent of resistance in *Schistosoma mansoni* populations is unknown. We examined
34 the genetic basis of variation in PZQ response in a *S. mansoni* population (SmLE-PZQ-R) selected with
35 PZQ in the laboratory: 35% of these worms survive high dose (73 µg/mL) PZQ treatment. We used genome
36 wide association to map loci underlying PZQ response. The major chr. 3 peak shows recessive inheritance
37 and contains a transient receptor potential (*Sm.TRPM_{PZQ}*) channel (Smp_246790), activated by nanomoles
38 of PZQ. Marker-assisted selection of parasites at a single *Sm.TRPM_{PZQ}* SNP enriched populations of PZQ-
39 R and PZQ-S parasites showing >377 fold difference in PZQ response. The PZQ-R parasites survived
40 treatment in rodents better than PZQ-S. Resistant parasites show 2.25-fold lower expression of
41 *Sm.TRPM_{PZQ}* than sensitive parasites. Specific chemical blockers of *Sm.TRPM_{PZQ}* enhanced PZQ
42 resistance, while *Sm.TRPM_{PZQ}* activators increased sensitivity. A single SNP in *Sm.TRPM_{PZQ}* differentiated
43 PZQ-ER and PZQ-ES lines, but mutagenesis showed this was not involved in PZQ-R, suggesting linked
44 regulatory changes. We surveyed *Sm.TRPM_{PZQ}* sequence variation in 259 individual parasites from the New
45 and Old World revealing one nonsense mutation, that results in a truncated protein with no PZQ binding
46 site. Our results demonstrate that *Sm.TRPM_{PZQ}* underlies variation in PZQ response in *S. mansoni* and
47 provides an approach for monitoring emerging PZQ-resistance alleles in schistosome elimination programs.

48

49 INTRODUCTION

50 Praziquantel (PZQ) is the drug of choice for treating schistosomiasis, a snail vectored parasitic disease,
51 caused by flatworms in the genus *Schistosoma*. Schistosomiasis is widespread: three main parasite species
52 infect over 140 million people in Africa, the Middle-East, South America and Asia (1, 2), resulting in
53 widespread morbidity – a global burden of 1.9 million disability adjusted life years (3) – and mortality
54 estimates ranging from 20 to 280 thousand annually (4, 5). Pathology results from eggs that lodge in the
55 liver and intestine (*S. mansoni* and *S. japonicum*) or in the urogenital system (*S. haematobium*) stimulating
56 granuloma formation. This results in a spectrum of pathology including portal hypertension, hepatosplenic
57 disease, bladder cancer, genital schistosomiasis and infertility. *S. mansoni* infection alone results in a
58 conservative estimate of 8.5 million cases of hepatosplenomegaly in sub-Saharan Africa (6). Mass drug
59 administration programs currently distribute an estimated 250 million doses of PZQ per year aimed in the
60 short term at reducing schistosome associated morbidity and mortality, and in the longer term at eliminating
61 schistosomiasis transmission (7, 8). PZQ is also widely used for treatment of other flatworm parasites of
62 both humans and livestock including tapeworms.

63 PZQ treatment of adult worms results in rapid Ca^{2+} influx into cells, muscle contraction and tegument
64 damage (9–12). Both the mechanism of action and the mechanism of resistance to PZQ have been the focus
65 for much speculation and research (13, 14). Several proteins like calcium gated channels (15–17) or ABC
66 transporters (18, 19) have been suspected to play a role in PZQ resistance. However, this topic has been
67 stimulated by the recent finding that a transient receptor channel (*Sm.TRPM_{PZQ}*) is activated by nanomolar
68 quantities of PZQ (20, 21).

69 Mass drug treatment with PZQ has enormous health benefits and has been extremely effective in reducing
70 parasite burdens and transmission (8), but imposes strong selection for resistance on treated schistosome
71 populations. Emergence of PZQ resistance is a major concern, because it could derail current progress
72 towards WHO goal of eliminating schistosomiasis as a public health problem by 2025 (8). Several lines of

73 evidence from both the field and the laboratory suggest that PZQ response varies in schistosome populations
74 (22–27). PZQ resistance is readily selected in the laboratory through treatment of infected rodents or
75 infected intermediate snail hosts (28). This typically results in a modest change (3-5 fold) in PZQ response
76 in parasite populations (28, 29), although the PZQ resistance status of individual worms comprising these
77 populations is unknown. PZQ treatment typically results in ~30% of patients who remain egg positive
78 following PZQ treatment (30). PZQ kills adult worms, but not immature parasites (31, 32), so both newly
79 emerging adult parasites and drug resistance may contribute to treatment failure. There have been several
80 reports of patients who remained egg positive across multiple PZQ treatment cycles (33, 34): schistosome
81 infections established in mice from infective larvae from these patients showed elevated resistance to PZQ
82 (24, 35). In Kenya and Uganda, infected communities where prevalence and disease burden are not reduced
83 by repeated treatment have been identified. The causes of these “hotspots” (36, 37) is currently unknown,
84 but PZQ-resistant schistosomes are one explanation. In a large longitudinal study of individual school age
85 children, egg reduction ratios (ERR) were high in naïve populations treated with PZQ, but showed a
86 significant decline after multiple rounds of treatment (38), consistent with selection of tolerance or
87 resistance to PZQ. Identification of molecular markers for direct screening of levels of PZQ resistance
88 alleles would be extremely valuable for parasite control programs, because changes in schistosome ERR
89 have both genetic and non-genetic explanations and are laborious to measure.

90 The availability of good genome sequence and near complete genome assembly (39) for *S. mansoni* make
91 unbiased genome wide approaches feasible for schistosome research (40). Our central goal is to determine
92 the genetic basis determinants of variation in PZQ response, using genome wide association approaches.
93 We exploit the PZQ-resistant parasites generated by laboratory selection (26) to determine the genetic basis
94 of PZQ, identifying a transient receptor channel as the cause of variation in PZQ response. The Transient
95 Receptor Potential Melastatin (TRPM) ion channel identified is activated by PZQ (20, 21) and has been
96 designated *Sm.TRPM_{PZQ}*. Together, our genetic analysis and the independent pharmacological analysis by

97 Park *et al.* (21) identify the target channel for PZQ and provide a framework for monitoring PZQ resistance
98 evolution in schistosome control programs.

99 RESULTS

100 PZQ resistant parasites are present in laboratory schistosome populations

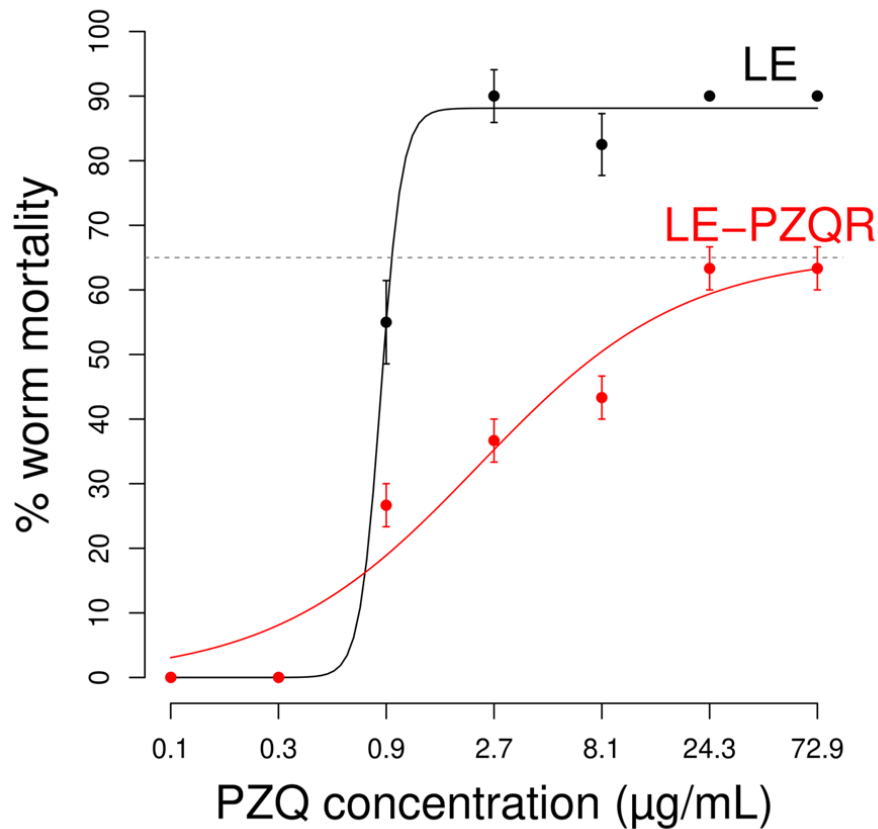


Fig. 1. Dose response curves for SmLE (PZQ-S) and the derived SmLE-PZQ-R (PZQ-R) populations. PZQ dose response curves show a ~14-fold difference in response between SmLE (ancestral population) and SmLE-PZQ (PZQ selected population) (χ^2 test = 10.387, $p = 0.001$). The PZQ-selected laboratory schistosome population (LE-PZQ-R) is polymorphic for drug response. 35% of SmLE-PZQ-R are not killed by treatment with high dose of PZQ, suggesting that this population is polymorphic ($N=240$ worms/parasite populations).

101 Male and female schistosome parasites pair in the blood vessels and reproduction is obligately sexual, so
102 schistosomes are maintained in the laboratory as outbred populations. Hence, individual parasites within
103 laboratory populations may vary in PZQ response. We measured PZQ response in the LE-PZQ-R
104 population, which was previously generated by PZQ treatment of infected snails (26). This revealed a 14-
105 fold difference in IC_{50} between the LE progenitor parasite population ($IC_{50}=0.86 \pm 0.14 \mu\text{g/mL}$) and LE-
106 PZQ-R ($IC_{50}=12.75 \pm 4.49 \mu\text{g/mL}$, χ^2 test, $p = 0.001$) derived by PZQ selection (Fig. 1). This is higher than
107 the 3-5 fold differences observed between PZQ-selected and unselected parasite populations in previous
108 studies (28). Interestingly, the dose response curve for the LE-PZQ-R population plateaus at 65% mortality:
109 the remaining 35% of parasites recovered even at high dose of PZQ (72.9 $\mu\text{g/mL}$). These results suggest
110 that the LE-PZQ-R parasite population is a mixed population that contains both PZQ-sensitive and PZQ-
111 resistant individual worms (Fig. 1).

112

113 **Association mapping of PZQ resistant genes identifies a TRPM channel**

114 We conducted a genome wide association study (GWAS) to determine the genetic basis of PZQ resistance
115 (PZQ-R). GWAS has been widely used for mapping drug resistance in parasitic protozoa (41) and the model
116 nematode *Caenorhabditis elegans* (42), but has not previously been applied to parasitic helminths, because
117 of the difficulty of accurately measuring drug response in individual parasites. When worms are treated
118 with PZQ, there is a massive influx of Ca^{2+} into cells and parasites contract (17, 43), but some worms
119 recover and resume respiration and movement 24-48h after drug removal. We assayed parasite recovery
120 following high dose PZQ treatment (24 $\mu\text{g/mL}$) of individual male worms maintained in 96-well plates by
121 measuring L-lactate production (44), a surrogate measure of respiration, 48h after PZQ treatment removal
122 (Fig. S1). These assays allow efficient measurement of recovery in individual PZQ-treated worms.

123 We conducted replicate experiments (A: $n = 590$; B: $n = 691$) to measure PZQ response in individual
124 parasites maintained in 96-well plates. The distributions of L-lactate production in the two experiments

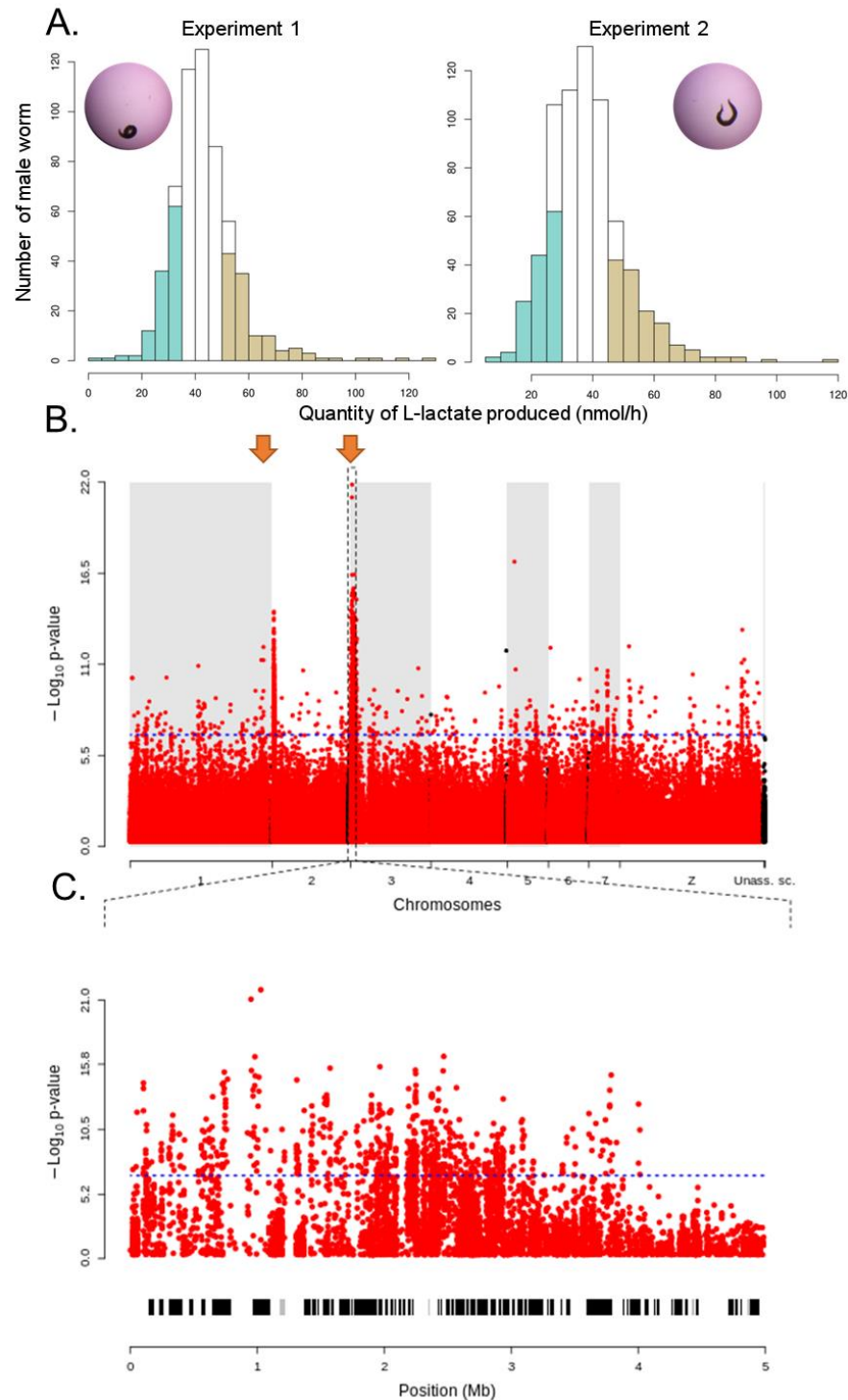


Fig. 2. Genome-wide association mapping of PZQ response. (A). We measured recovery of individual adult male worms following expose to 24 μ g/mL PZQ by measuring lactate production. The distribution from both experimental replicates is shown (A: $N=590$; B: $N=691$). Worms in the bottom and top quintile were each pooled, and genome sequenced to high read depth. (B). The Manhattan plot identifies genome regions that differ in allele frequency between high and low lactate worm pools. (C). The chr. 3 QTL identified spans 4 Mb and 91 genes, including several promising candidates.

126 were broad (A: 0-126.56 nmol/h, mean = 42.95 nmol/h; B: 0-118.61 nmol/h, mean = 37.79 nmol/h): we
127 identified worms from the top and bottom quintile for lactate production (Fig. 2A) which were then bulk
128 sequenced to high read depth (average read depth - A: 39.97; B: 36.83). Two genome regions (chr. 2 and
129 chr. 3) showed strong differentiation in allele frequencies between parasite populations showing high and
130 low lactate production phenotypes (Fig. 2B). The highest peak ($p = 1.41 \times 10^{-22}$) on chr. 3 spanned 4 Mb
131 (22,805-4,014,031 bp) and contained 91 genes, of which 85 are expressed in adult worms (Fig. 2C). This
132 genome region contains several potential candidate loci including three partial ABC transporters (Table
133 S1). One gene close to the highest association peak is of particular interest: Smp_246790 is a transient
134 receptor potential channel in the M family (TRPM). This same channel was recently shown to be activated
135 by PZQ following exposure to nM quantities of drug resulting in massive Ca^{2+} influx into HEK293 cells
136 transiently expressing this protein (20, 21). This gene, designated *Sm.TRPM_{PZQ}*, is therefore a strong
137 candidate to explain variation in PZQ response within parasite populations. Two other features of the data
138 are of interest. First, the SNP (position 1029621 T>C) marking the highest association peak (at 1,030 Mb)
139 is found in a transcription factor (Smp_345310, SOX13 homology) from a family known to regulate
140 splicing variants (45). Second, there is a ~100 kb deletion (1220683- 1220861 bp) 6.5 kb from *Sm.TRPM_{PZQ}*
141 and another 150 kb deletion (1,200,000-1,350,000 bp) 170 kb from the transcription factor. This was
142 enriched in high lactate groups in both replicates and is in linkage disequilibrium with the enriched SNP in
143 *Sm.TRPM_{PZQ}*.

144 The chr. 2 peak ($p < 1.0 \times 10^{-15}$) spans 1.166 Mb (291,191-1,457,462 bp) and contains 24 genes (21
145 expressed in adult worms). This genome region contains no genes that could be a candidate to explain
146 variation in PZQ response.

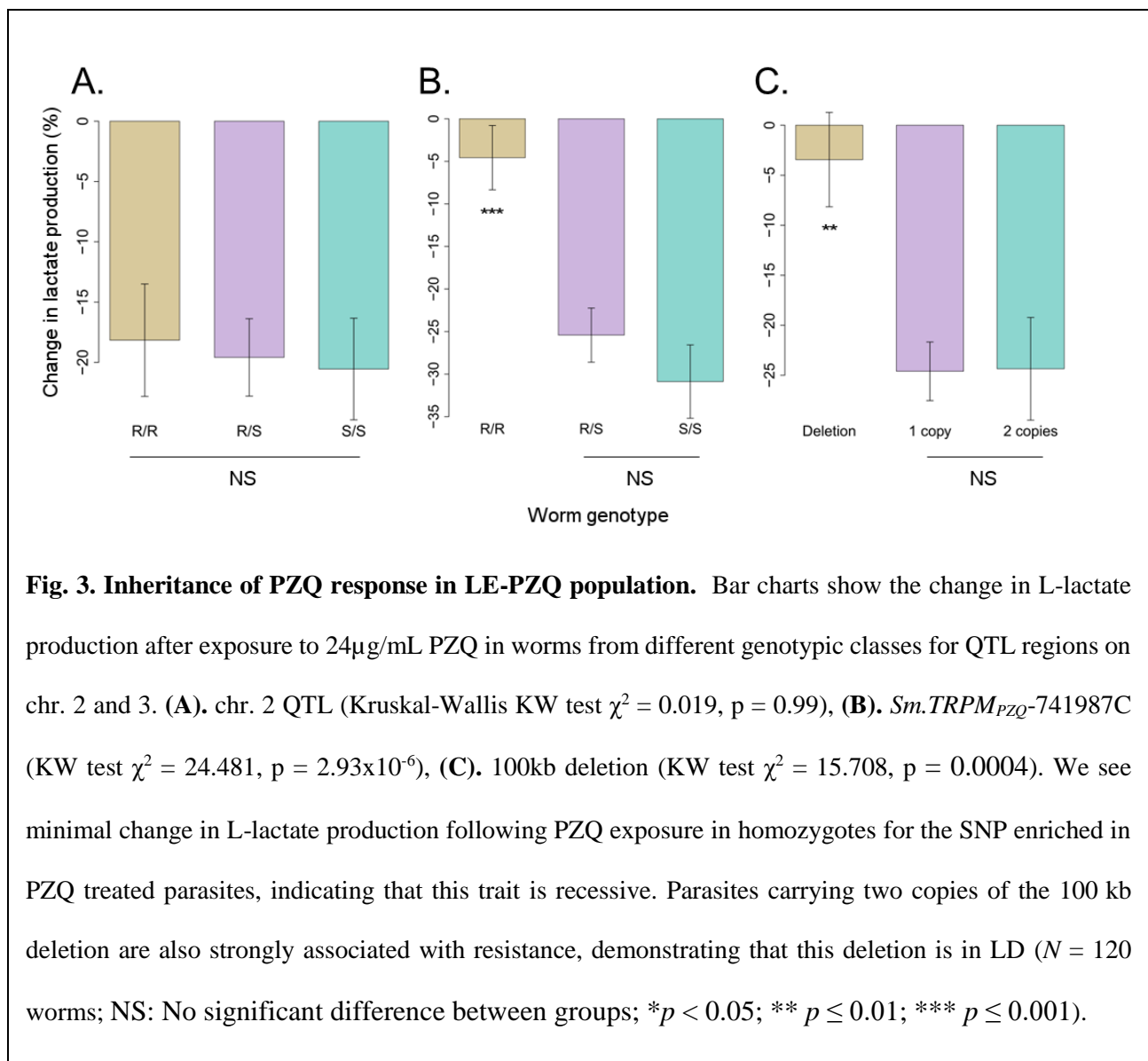
147

148

149

150 **PZQ resistance shows recessive inheritance**

151 To confirm these associations and determine whether the loci underlying PZQ response are inherited in a
152 dominant, co-dominant or recessive manner, we compared genotype and PZQ-response phenotypes in
153 individual worms. We compared the L-lactate production phenotypes of individual worms maintained in
154 96-well plates 48 hours after exposure to 24 $\mu\text{g}/\text{mL}$ PZQ with their genotypes at SNPs at the peaks of the
155 chr. 2 and chr. 3 QTLs. We also examined copy number of one of the 100 kb deletion observed on chr. 3
156 using qPCR. We observed significant differences in L-lactate production among genotypes (Fig. 3). Both



157 the copy number variant and the SNP assayed in *Sm.TRPM_{PZQ}* revealed that the causative gene in the chr.
158 3 QTL showed recessive inheritance. Homozygous parasites carrying two copies of the *Sm.TRPM_{PZQ}*-
159 741987C allele (or two copies of the deletion) recovered from PZQ treatment, while the heterozygote and
160 other homozygotes failed to recover from treatment (Fig. 3B-C). For the chr. 2 QTL, we did not see a
161 significant association between parasite genotype and PZQ-R phenotype nor with lactate production before
162 PZQ treatment (Fig. 3A): this locus was not investigated further.

163

164 **Marker-assisted purification of resistant and sensitive parasites**

165 As the chr. 3 QTL containing *Sm.TRPM_{PZQ}* shows the strongest association with PZQ response and shows
166 recessive inheritance, we were able to use single generation marker assisted selection approach to enrich
167 parasites for alleles conferring PZQ resistance (PZQ-R) and PZQ sensitivity (PZQ-S) from the mixed
168 genotype LE-PZQ-R parasite population (Fig. 4A). We genotyped cercariae larvae emerging from snails
169 previously exposed to single miracidia to identify parasites homozygous for the recessive PZQ-R allele
170 from those homozygous for the PZQ-S allele. Parasites isolated from multiple snails falling into these two
171 alternative genotypes were then used to infect hamsters. The enriched PZQ-resistant and sensitive parasites
172 were designated SmLE-PZQ-ER and SmLE-PZQ-ES. Sequencing of adult parasites recovered from these
173 two populations revealed that they were fixed for alternative alleles at the *Sm.TRPM_{PZQ}*-741987C SNP
174 genotyped, but showed similar allele frequencies across the rest of the genome (Fig. S2). As expected, these
175 sequences also revealed that the 100 kb deletion was close to fixation in the SmLE-PZQ-ER population
176 (Fig. S3).

177 We conducted PZQ dose response curves on these enriched parasite populations. The SmLE-PZQ-ES
178 population had an IC₅₀ of 0.193 µg/mL (± 1 s. d.: 0.045), while the SmLE-PZQ-ER population did not reach
179 50% reduction even at the highest dose (72.9 µg/mL) so has an IC₅₀ >72.9 µg/mL: the two purified
180 populations differ by >377-fold in PZQ response (Fig. 4B). These results provide further demonstration

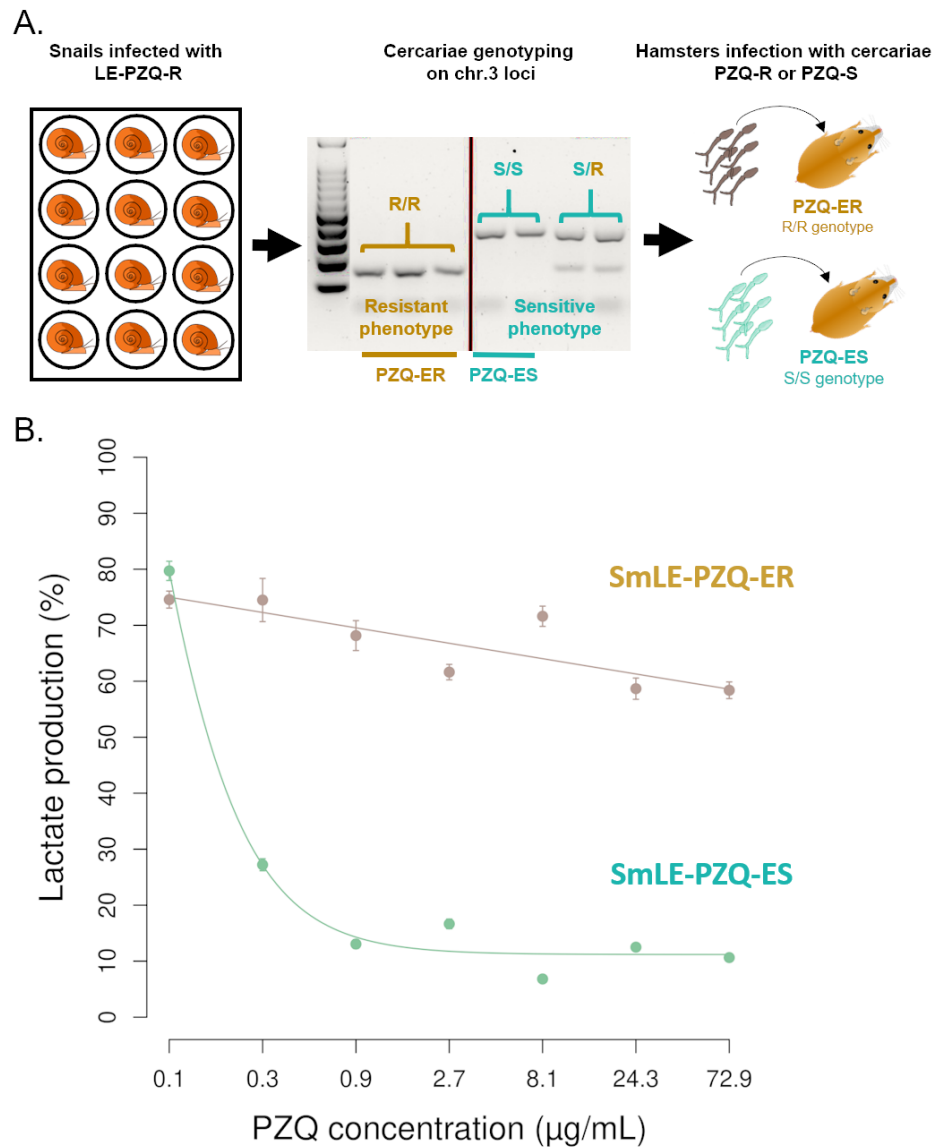


Fig. 4. Single generation marker-assisted purification of SmLE-PZQ-ES and SmLE-PZQ-ER parasites.

(A). Experimental strategy for identifying parasite larvae that are homozygous for *Sm.TRPM_{PZQ}* alleles associated with PZQ-R or PZQ-S. We genotyped cercaria larvae emerging from snails infected with single parasite genotypes for a restriction site in the *Sm.TRPM_{PZQ}* gene, and then infected two groups of hamsters with parasites homozygous for alternative alleles at this locus. (B). The two populations of parasites generated show dramatic differences in PZQ-response ($N = 60$ worms/population/treatment, χ^2 test = 373.03, $p < 2.2 \times 10^{-16}$).

182 that the original LE-PZQ-R parasite population was a mixture of PZQ-R and PZQ-S parasites. Separation
183 of the component SmLE-PZQ-ES and SmLE-PZQ-ER parasites from these mixed populations allows
184 rigorous characterization of the PZQ-R trait in parasite populations that are fixed for alternative alleles at
185 *Sm.TRPM_{PZQ}*, but contain comparable genomic backgrounds across the rest of the genome.

186

187 ***Sm.TRPM_{PZQ}* gene and isoform expression is reduced in SmLE-PZQ-ER parasites**

188 PZQ response varies between parasite stages and sexes, with strongest response in adult males. Adult
189 females and juvenile worms are naturally resistant (31, 32). We therefore examined gene expression in the
190 purified SmLE-PZQ-ES and SmLE-PZQ-ER populations (males and females for both adults and juvenile
191 worms) using RNA-seq (Fig. 5). Of the 85 genes expressed in adult worms under the chr. 3 QTL, only the
192 *Sm.TRPM_{PZQ}* showed a significant reduction in expression in the SmLE-PZQ-ER adult male worms relative
193 to SmLE-PZQ-ES (2.25-fold, posterior probability = 1) (Fig. 5A-B). Comparable under expression of
194 *Sm.TRPM_{PZQ}* was also seen in female when compared to SmLE-PZQ-ES: expression of *Sm.TRPM_{PZQ}* was
195 11.94-fold lower in female than in male worms, consistent with females being naturally resistant (31, 32)
196 (Fig. 5C). However, juvenile male and female worms showed elevated gene expression compared with
197 adult worms (Fig. 5C). This is surprising because juveniles are naturally resistant to PZQ. *Sm.TRPM_{PZQ}* has
198 41 exons and occurs as 7 isoforms containing between 3 and 36 exons. Strikingly, SmLE-PZQ-ES male
199 worms showed a 4.02-fold higher expression of isoform 6 compared to SmLE-PZQ-ER males, and an 8-
200 fold higher expression than naturally resistant juvenile worms from both populations (while SmLE-PZQ-
201 ER showed only a 2-fold higher expression) (Fig. 5B and D and Fig. S4). This suggests that high expression
202 of isoform 6 is linked to PZQ sensitivity. The 15 exons of isoform 6 produce an 836 amino acid protein that
203 lacks the transmembrane domain but contains the TRPM domain. We interrogated the 10x single cell
204 expression data from adult worms (46) showing that *Sm.TRPM_{PZQ}* is expressed mainly in neural tissue with
205 some expression also in muscle (Fig. S5).

206

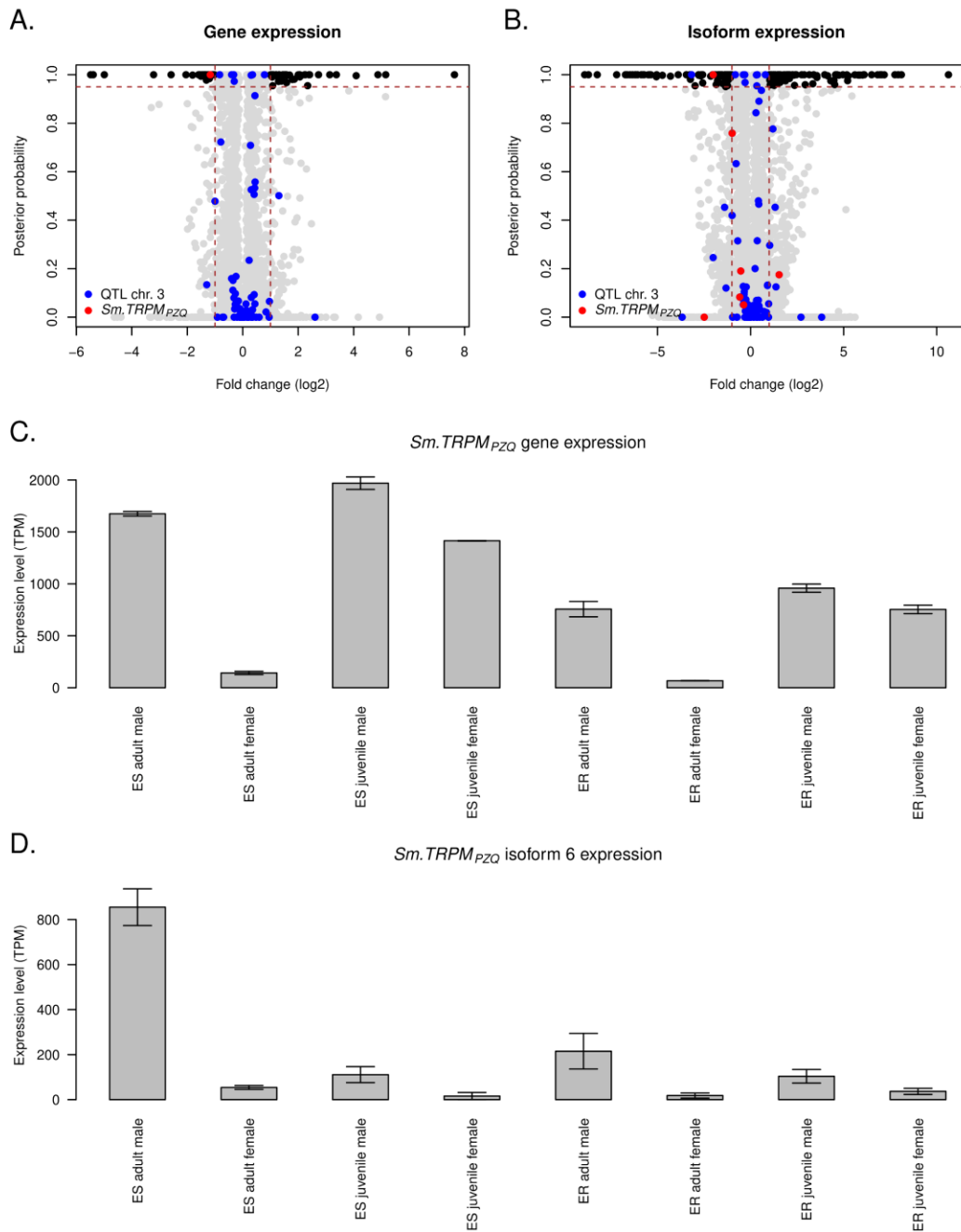
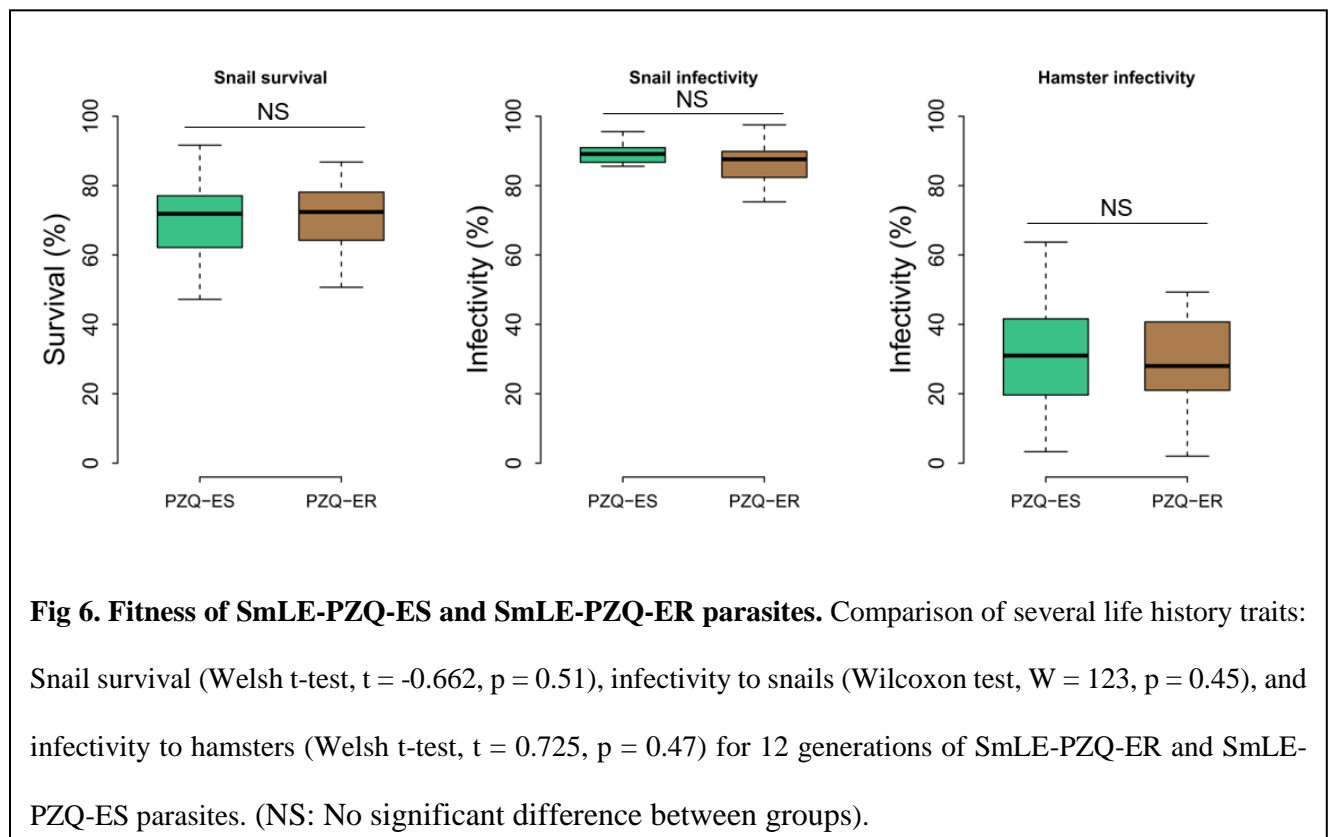


Fig. 5. Gene expression differences between *SmLE-PZQ-ES* and *SmLE-PZQ-ER* parasites. Volcano plot showing the differential (A). gene expression and (B). isoform expression between adult male PZQ-ES and PZQ-ER (In blue: genes located under the chr. 3 QTL, in red: *Sm.TRPM_{PZQ}* gene). (C). *Sm.TRPM_{PZQ}* gene expression and (D). *Sm.TRPM_{PZQ}* isoform 6 expression level comparison between PZQ-ES and ER for the two sex (i.e. male and females) and different stages (i.e. adult and juvenile). High expression of *Sm.TRPM_{PZQ}* isoform 6 is linked to PZQ sensitivity.

207 **Fitness of SmLE-PZQ-ER and SmLE-PZQ-ES parasite populations**

208 Both laboratory selected and field isolated *S. mansoni* showing PZQ-R have been difficult to maintain in
209 the laboratory (47): the PZQ-R trait has been rapidly lost consistent with strong selection against this trait.
210 It has been suggested that PZQ-R carries a fitness cost that will slow spread of this trait in the field under
211 PZQ pressure. Such fitness costs are a common, but not ubiquitous, feature of drug resistance in other
212 pathogens (48–50). We measured several components of parasite fitness in SmLE-PZQ-ES and SmLE-
213 PZQ-ER parasites during laboratory passage of purified parasite lines, but found no significant differences
214 in infectivity to snails, snail survival, or infectivity to hamsters (Fig. 6A). We did not see loss of PZQ-R in
215 our lines after 12 generations because the key genome region is fixed. Cioli *et al.* (28) has also reported



216 long term stability of PZQ-R parasite populations indicative that PZQ-R associated fitness costs maybe
217 limited or absent.

218

219 ***In vivo* efficacy of PZQ against SmLE-PZQ-ES and SmLE-PZQ-ER parasites**

220 To determine the relationship between *in vitro* PZQ-R measured in 96-well plates, and *in vivo* resistance,
221 we treated mice infected with either SmLE-PZQ-ER or SmLE-PZQ-ES parasites populations with
222 120 mg/kg of PZQ. We observed no significant reduction in worm burden in SmLE-PZQ-ER parasites
223 when comparing PZQ-treated and control (DMSO) treated animals (Wilcoxon test, $p = 0.393$; Fig. S6A).
224 In contrast, we recovered significantly lower numbers of worms from PZQ-treated versus untreated mice
225 infected with the SmLE-PZQ-ES parasite population (Wilcoxon test, $p = 0.008$; Fig. S6A). The percent
226 reduction observed was significantly different between the SmLE-PZQ-ES and SmLE-PZQ-ER parasites
227 (Wilcoxon test, $p = 0.0129$; Fig. S6B). Interestingly, we observed a large reduction in numbers of female
228 worms recovered from PZQ-treated SmLE-PZQ-ES parasites relative to untreated animals (Wilcoxon test,
229 $p = 0.008$; Fig. S6D), while for male worms this did not reach significance (Wilcoxon test, $p = 0.089$, Fig.
230 S6C). We saw no impact of PZQ-treatment for either female or male worms in mice infected with SmLE-
231 PZQ-ER. These results show that *in vivo* PZQ response in treated mice differs between SmLE-PZQ-ES and
232 SmLE-PZQ-ER parasites. These data also suggest that the extended paralysis of male SmLE-PZQ-ES
233 worms under PZQ treatment may reduce their ability to maintain female worms *in copula*.

234

235 **Chemical blockers and activators of *Sm.TRPM_{PZQ}* modulate PZQ-R**

236 *Sm.TRPM_{PZQ}* emerges as a strong candidate gene to explain variation in PZQ response, but validation is
237 required. We were unsuccessful in knocking down expression of *Sm.TRPM_{PZQ}* using either siRNA or
238 dsRNA (Table S2), possibly because this gene is expressed mainly in neural tissue. We therefore used two

239 chemical modulators of Sm.TRPM_{PZQ} activity – an *Sm.TRPM_{PZQ}* agonist (AG1) and Sm.TRPM_{PZQ}
240 antagonist (ANT1). These were identified from a screen of ~16,000 compounds by screening Ca²⁺ influx
241 into HEK293 cells transiently expressing Sm.TRPM_{PZQ} (Chulkov *et al.*, in prep). Addition of the
242 Sm.TRPM_{PZQ} blocker (antagonist ANT1) allowed SmLE-PZQ-ES worms to recover from PZQ treatment
243 (Fig. 7A), while the Sm.TRPM_{PZQ} activator (agonist AG1) rendered SmLE-PZQ-ER worms sensitive to
244 PZQ treatment in a dose dependent manner (Fig. 7B). These results are consistent with a role for
245 Sm.TRPM_{PZQ} in determining variation in PZQ response.

246 We found 5 non-synonymous SNPs and 5 insertions that showed significant differences in allele frequency
247 in *Sm.TRPM_{PZQ}* in the SmLE-PZQ-ES and SmLE-PZQ-ER parasite populations. One of these SNPs
248 (*Sm.TRPM_{PZQ}*-741903) and two insertions (*Sm.TRPM_{PZQ}*-779355 and *Sm.TRPM_{PZQ}*-779359) are fixed for
249 alternative alleles in the two populations, with 7 others are segregating at different frequencies in the two
250 populations (Fig. S3). These SNPs are located outside the critical transmembrane domains so were not
251 strong candidates to explain differences in PZQ-R. We expressed *Sm.TRPM_{PZQ}* carrying some of these
252 variants in HEK293 cells and examined their impact on Ca²⁺ influx to interrogate their role in explaining

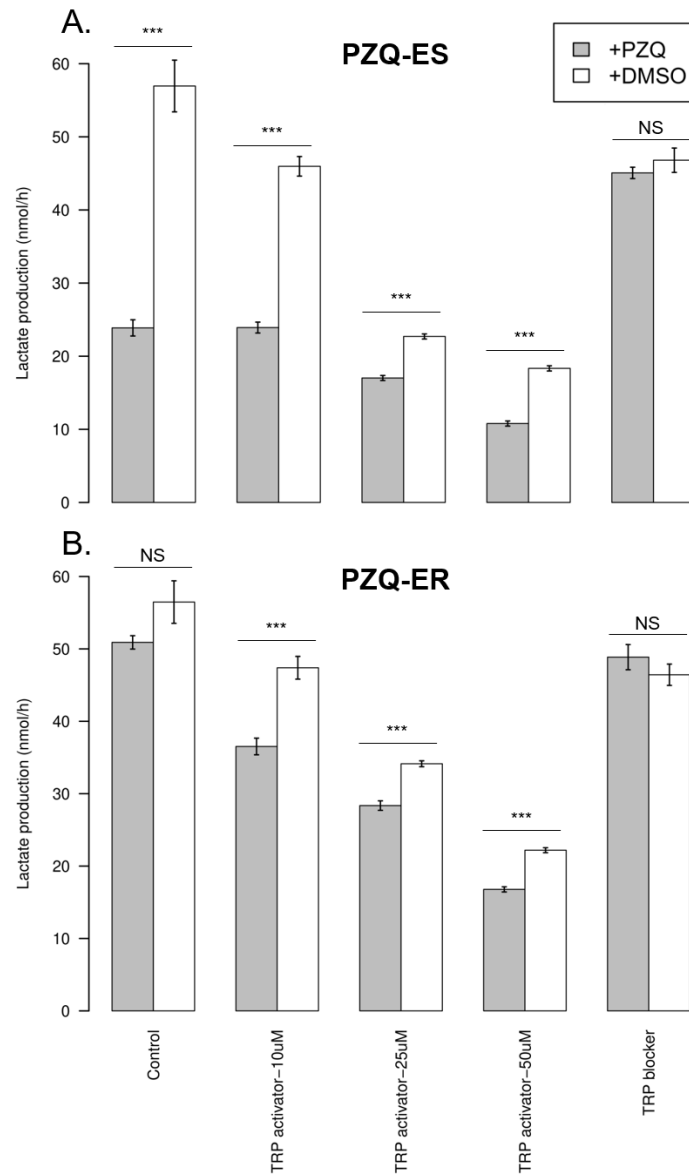


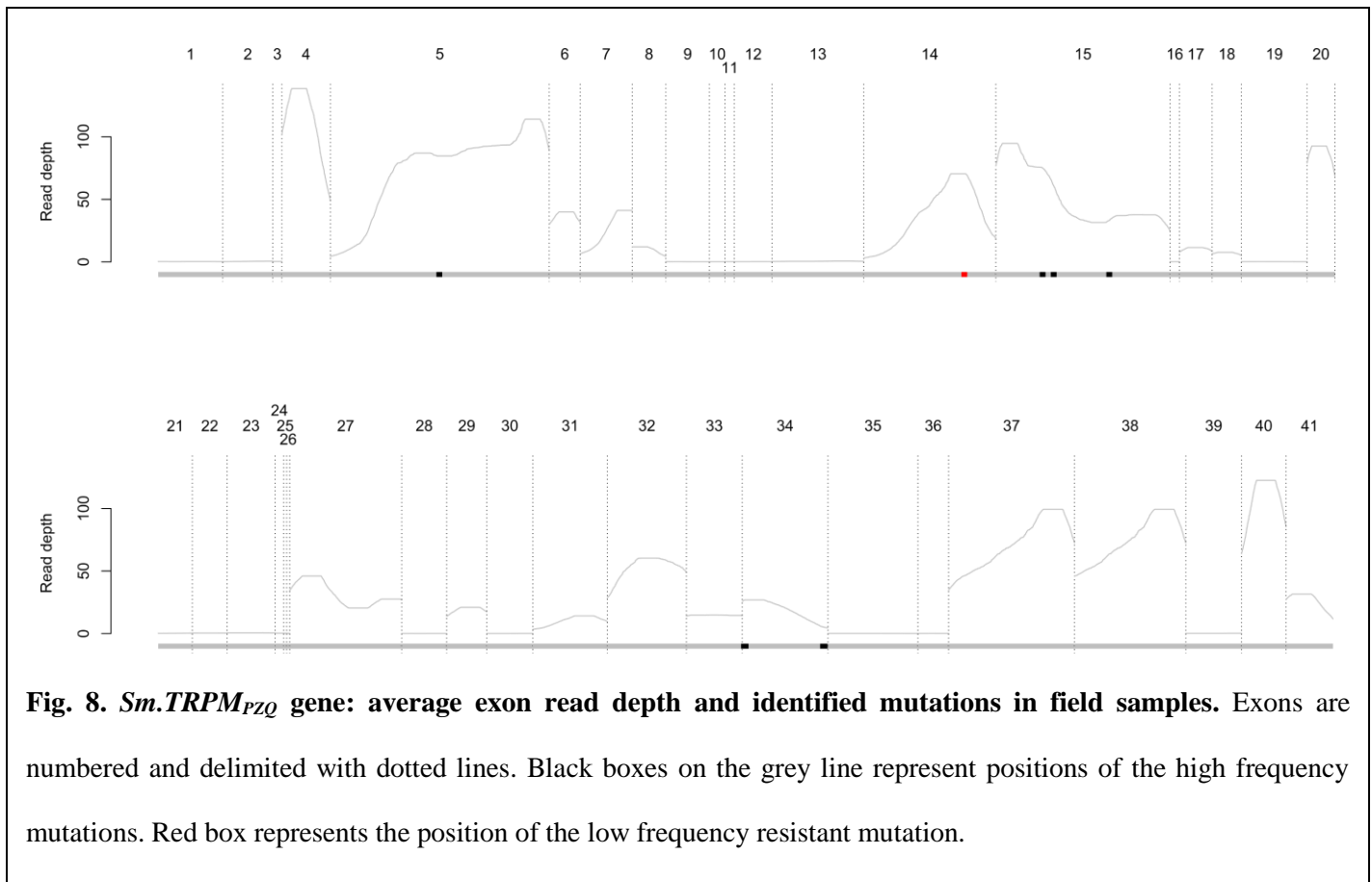
Fig. 7. Impact of *Sm.TRMP_{PZQ}* blockers and activators on PZQ response. (A) SmLE-PZQ-ES and (B) SmLE-PZQ-ER were exposed to either i) PZQ or DMSO alone (control group), ii) PZQ or DMSO combined with either 10 μ M, 25 μ M or 50 μ M of *Sm.TRMP_{PZQ}* activator (agonist AG1), iii) PZQ or DMSO combined with 50 μ M *Sm.TRMP_{PZQ}* blocker (antagonist ANT1). Parasite viability was assessed 3 days post-treatment, based on their L-lactate production). Addition of the *Sm.TRMP_{PZQ}* blocker allowed SmLE-PZQ-ES worms to recover from PZQ treatment (Welsh t-test, $t = -0.94$, $p = 0.35$), while the *Sm.TRMP_{PZQ}* activator (agonist AG1) rendered SmLE-PZQ-ER worms sensitive to PZQ treatment in a dose dependent manner (N = 20 worms/population/treatment; Welsh t-test, NS: No significant difference between groups; * $p < 0.05$; ** $p \leq 0.01$; *** $p \leq 0.001$.)

254 underlie PZQ response. We speculate that the difference in PZQ response is due to expression patterns and
255 may be controlled by regulatory variants potentially associated with the adjacent 100 kb deletion or the
256 SOX13 transcription factor.

257

258 **Sequence variation in *Sm.TRPM_{PZQ}* from natural *S. mansoni* populations**

259 Methods for evaluating frequencies of PZQ-resistance mutations in endemic regions would provide a
260 valuable tool for monitoring mass treatment programs aimed at schistosome elimination. Both this paper
261 and the accompanying paper (21) identify *Sm.TRPM_{PZQ}* as being critical to PZQ-response, and Park *et al.*
262 have determined critical residues that determine binding between PZQ and *Sm.TRPM_{PZQ}* (21). We
263 examined the mutations present in *Sm.TRPM_{PZQ}* in natural schistosome populations using exome



264 sequencing from 259 miracidia, cercariae or adult parasites from 3 African countries (Senegal, Niger,
265 Tanzania), the Middle East (Oman) and South America (Brazil) (51, 52). We were able to sequence 36/41
266 exons of *Sm.TRPM_{PZQ}* from 122/259 parasites on average (s.e. = 18.65) (Table S3). We found 1 putative
267 PZQ-R SNP in our Illumina reads supported by a very high coverage (Fig. S7). This SNP (c.2708G>T on
268 isoform 5, p.G903*) was found in a single Omani sample and resulted in a truncated protein predicted to
269 result in loss-of-function, demonstrating that PZQ-R alleles are present in natural populations. However,
270 this PZQ-R allele observed was rare and present in heterozygous state so would not impact PZQ response
271 (Fig. 8).

272

273 **DISCUSSION**

274 Our genetic approach to determining the genes underlying PZQ resistance – using GWAS and a simple
275 lactate-based read out to determine parasite recovery following PZQ treatment in individual parasites –
276 robustly identifies a TRPM channel (*Sm.TRPM_{PZQ}*) as the cause of variation in PZQ response. We were
277 further able to purify SmLE-PZQ-ER and SmLE-PZQ-ES parasites to examine drug response and gene
278 expression and to use chemical blockers to directly implicate *Sm.TRPM_{PZQ}*. Our results complement those
279 of Park *et al.* (21) who used a pharmacological approach to determine that *Sm.TRPM_{PZQ}* is the major target
280 for PZQ, and identified the critical residues necessary for activation by PZQ. Together, these approaches
281 demonstrate that TRPM is a key determinant of schistosome response to PZQ.

282 A striking feature of the results is the strength of the PZQ-R phenotype. While previous authors have
283 described quite modest differences (3-5 fold) in PZQ-response among *S. mansoni* isolates (28, 29), this
284 study revealed at least 377-fold difference in IC₅₀ between SmLE-PZQ-ER and SmLE-PZQ-ES parasites.
285 These large differences were only evident after we used marker-assisted selection to divide a mixed
286 genotype laboratory *S. mansoni* population into component SmLE-PZQ-ER and SmLE-PZQ-ES
287 populations. The modest IC₅₀ differences in previous studies observed are most likely because the parasite

288 lines compared contained mixed populations of both SmLE-PZQ-ER and SmLE-PZQ-ES individuals. This
289 highlights a critical feature of laboratory schistosome populations that is frequently ignored: these
290 populations are genetically variable and contain segregating genetic and phenotypic variation for a wide
291 variety of parasite traits. In this respect they differ from the clonal bacterial or protozoan parasite “strains”
292 used for laboratory research. Importantly, we can use this segregating genetic variation for genetic mapping
293 of biomedically important parasite traits such as PZQ resistance.

294 There is strong evidence that PZQ-R parasites occur in schistosome populations in the field, but the
295 contribution of PZQ-R to treatment failure in the field are unclear. Molecular markers are widely used for
296 monitoring changes in drug resistance mutations in malaria parasites (53–55) and for evaluating
297 benzimidazole resistance in nematode parasites of veterinary importance (56, 57). The discovery of the
298 genetic basis of resistance to another schistosome drug (oxamniquine) (58) now makes genetic surveys
299 possible to evaluate oxamniquine resistance in schistosome populations (52, 59). Identification of
300 *Sm.TRPM_{PZQ}* as a critical determinant of PZQ response, and determination of key residues that can underlie
301 PZQ-R, now makes molecular surveillance possible for *S. mansoni*. We examined variation in *Sm.TRPM_{PZQ}*
302 in 259 parasites collected from locations from across the geographical range of this parasite. We were
303 unable to confirm mutations in any of the key residues that block PZQ binding identified in the mutagenesis
304 studies by Park *et al.* (21). However, we identified a stop codon in a single parasite isolated from a rodent
305 from Oman (60) indicating a low frequency of PZQ-R resistance alleles (1/502, frequency = 0.002). This
306 stop codon was in heterozygous state so is unlikely to result in PZQ-R.

307 These results are extremely encouraging for control programs, but should be viewed with considerable
308 caution for two reasons. First, we do not know yet the regulatory regions of *Sm.TRPM_{PZQ}* and we were
309 unable to identify regulatory variants of *Sm.TRPM_{PZQ}* in this screen. Such variants could reduce expression
310 of *Sm.TRPM_{PZQ}* resulting in PZQ resistance. We note that coding variants underlying PZQ-R phenotype
311 were not found in our laboratory SmLE-PZQ-ER parasites, suggesting that regulatory changes may underlie
312 this trait. Second, *Sm.TRPM_{PZQ}* is a large gene (120 kb and 41 exons) that is poorly captured by genome

313 sequencing of field samples. We were able to successfully sequence 36/41 exons, including those that
314 directly interact with PZQ (21), using exome capture methods (51, 52). However, improved sequence
315 coverage will be needed for full length sequencing of this gene. Third, the parasite samples we examined
316 did not come from hotspot regions where regular mass drug administration of PZQ has failed to reduce *S.*
317 *mansoni* burdens (36, 61). Targeted sequencing of miracidia from these populations will be extremely
318 valuable to determine if there are local elevations in *Sm.TRPM_{PZQ}* variants, or if particular variants are
319 enriched in parasites surviving PZQ treatment. Ideally, such sequence surveys should be partnered with
320 functional validation studies in which variant *Sm.TRPM_{PZQ}* are expressed in HEK293 cells to determine
321 their response to PZQ exposure (21).

322

323 **MATERIALS AND METHODS**

324 **Study design**

325 This study was designed to determine the genetic basis of PZQ-R, and was stimulated by the initial
326 observation that a laboratory *S. mansoni* population generated through selection with PZQ contained both
327 PZQ-S and PZQ-R individuals. The project had 6 stages:(i) QTL location. We conducted a genome-wide
328 association study (GWAS). This involved measuring the PZQ-response of individual worms, pooling those
329 showing high levels of resistance and low levels of resistance, sequencing the pools to high read depth, and
330 then identifying the genome regions showing significant differences in allele frequencies between high and
331 low resistance parasites. (ii) Fine mapping of candidate genes. We identified potential candidate genes in
332 these QTL regions, through examination of gene annotations, and exclusion of genes that are not expressed
333 in adults. We also determined whether the loci determining PZQ-R are inherited in a recessive, dominant
334 or co-dominant manner (iii) Marker assisted purification of PZQ-S and PZQ-R parasites. To separate PZQ-
335 R and PZQ-S parasites into “pure” populations, we genotyped larval parasites for genetic markers in the
336 QTL regions and infected rodents with genotypes associated with PZQ-R or PZQ-S. To verify that this

337 approach worked, we then measured the IC₅₀ for each of the purified populations. (iv) Characterization of
338 purified SmLE-PZQ-ER and SmLE-PZQ-ES populations. Separation of SmLE-PZQ-ES and SmLE-PZQ-
339 ER parasite populations allowed us to characterize these in more detail. Specifically, we measured
340 expression in juvenile and adult worms of both sexes in both SmLE-PZQ-ES and SmLE-PZQ-ER parasites.
341 We also quantified parasite fitness traits. (v) Functional analysis. We used RNAi and chemical manipulation
342 approaches to modulate activity of candidate genes and determine the impact of PZQ-resistance. We also
343 used transient expression of candidate genes in cultured mammalian cells, to determine the impact of
344 particular SNPs on response to PZQ-exposure. (vi) Survey of PZQ-resistance variants in field collected
345 parasites. Having determined the gene underlying PZQ-R in laboratory parasites, we examined sequence
346 variation in this gene in a field collection of *S. mansoni* parasites collected to examine the frequency of
347 sequence variants predicted to result in PZQ-resistance. Methods are described in detail (File S1) and in
348 brief below.

349 Ethics statement

350 This study was performed following the Guide for the Care and Use of Laboratory Animals of the National
351 Institutes of Health. The protocol was approved by the Institutional Animal Care and Use Committee of
352 Texas Biomedical Research Institute (permit number: 1419-MA and 1420-MU). Ethical permission for
353 collection of samples from humans are described in (51, 52).

354

355 **Biomphalaria glabrata snails and Schistosoma mansoni parasites**

356 We used uninfected inbred 8 - 10 mm albino *Biomphalaria glabrata* snails (line Bg121 (62)). The SmLE
357 *S. mansoni* population was originally obtained from an infected patient in Brazil (63). The SmLE-PZQ-R
358 schistosome population was generated by applying a single round of PZQ selection pressure on SmLE
359 parasites at both snail and rodent stages (26) and has been maintained in our laboratory since 2014.

360

361 **Drug resistance tests:**

362 *Dose-response curves to PZQ in SmLE and SmLE-PZQ-R populations*

363 We initially measured PZQ sensitivity by examining worm motility (64) in SmLE and SmLE-PZQ-R
364 parasite populations. Ten adult males from SmLE or SmLE-PZQ-R populations were placed into each well
365 of a 24-well microplate containing 1 mL DMEM complete media (65). We performed control and
366 experimental groups in triplicate ($N=240$ worms/parasite population). We exposed adult worms to PZQ (0,
367 0.1 0.3, 0.9, 2.7, 8.1, 24.3 and 72.9 $\mu\text{g}/\text{mL}$) for 24h. Worms were washed (3x) in drug-free medium and
368 incubated (37°C , 5% CO_2) for 2 days. The parasites were observed daily for the 5 days and the number of
369 dead worms scored. Worms were defined as “dead” if they showed no movements and became opaque.

370

371 *Metabolic assessment of worm viability using L-lactate assay*

372 We adapted a method for metabolic assessment of worm viability using an L-lactate assay (44). Adult male
373 SmLE-PZQ-R worms were placed individually in 96-well plates containing 100 μm mesh filter insert
374 (Millipore) in 250 μL DMEM complete media. We added PZQ (24.3 $\mu\text{g}/\text{mL}$ in DMEM complete media)
375 while controls were treated with the same volume of drug diluent DMSO. At 48h post-treatment, the
376 supernatant (125 μL) was collected from each well and immediately stored at -80°C until processing. We
377 measured lactate levels in the supernatants of *in vitro* treated adult male worms with a colorimetric L-lactate
378 assay kit (Sigma) using 96-well, optical clear-bottom plates (Corning).

379

380 **Genome wide association analysis and QTL mapping**

381 *Schistosome infections*

382 We collected eggs from livers of hamsters infected with SmLE-PZQ-R (66) and exposed one thousand
383 Bg121 snails to five miracidia/snail. After 30 days, snails were individually exposed to light to shed
384 cercariae. We exposed eight hamsters to 840 cercariae (4 cercariae/snail) from a batch of 210 shedding
385 snails. We euthanized hamsters after 45 days to collect adult worms.

386

387 *Phenotypic selection*

388 We plated adult SmLE-PZQ-R males individually in 96-well plates (60 worms per plate) in 250 μ L of
389 DMEM complete media and treated with a 24.3 μ g/mL PZQ. A group of 12 worms was treated with the
390 same volume of drug diluent DMSO. This GWAS experiment was done twice independently. A total of
391 590 and 691 adult male worms were collected, cultured *in vitro* and exposed to PZQ for the two
392 experiments.

393 We collected media supernatants (125 μ L) in 96-well PCR plates after 24h in culture (pre-treatment)
394 and 48h post-treatment for quantifying lactate levels. We took the 20% of the treated worms releasing the
395 highest amount of lactate (average L-lactate production \pm SD: Experiment 1 = 61.44 nmol/h \pm 13.16 /
396 Experiment 2 = 56.38 nmol/h \pm 10.82) and the 20% of the treated worms releasing the lowest amount of
397 lactate (average L-lactate production \pm SD: Experiment 1 = 28.61 nmol/h \pm 5.32 / Experiment 2 = 23.04
398 nmol/h \pm 4.14), 48h post PZQ treatment.

399

400 DNA extraction and library preparation

401 We sequenced whole genomes of the two pools of recovered (Experiment 1: 116 worms / Experiment 2:
402 137 worms) and susceptible worms (Experiment 1: 116 worms / Experiment 2: 137 worms) and measured
403 allele frequencies in each pool to identify genome regions showing high differentiation. We extracted
404 gDNA from pools of worms (Blood and Tissue kit, Qiagen) and prepared whole genome libraries in
405 triplicate (KAPA HyperPlus kit, KAPA Biosystems). Raw sequence data are available at the NCBI
406 Sequence Read Archive (PRJNA699326).

407

408 Bioinformatic analysis

409 We used Jupyter notebook and scripts used for processing the sequencing data and identifying the QTL
410 (https://github.com/fdchevalier/PZQ-R_DNA).

411 a. *Sequence analysis and variant calling*

412 We (i) aligned the sequencing data against the *S. mansoni* reference genome using BWA (67) and SAMtools
413 (68), (ii) used GATK (69, 70) to mark PCR duplicates and recalibrate base scores, (iii) used the

414 HaplotypeCaller module of GATK to call variants (SNP/indel) and GenotypeGVCFs module to perform
415 joint genotyping. We merged VCF files using the MergeVcfs module. All steps were automated using
416 Snakemake (71).

417 b. *QTL identification*

418 We examined the difference in allele frequencies between low and high lactate parasites across the genome
419 by calculating a Z-score at each bi-allelic site. We weighed Z-scores by including the number of worms in
420 each treatment and the difference in the total read depth across the triplicated libraries of each treatment at
421 the given variant. We combined Z-scores generated from each biological replicate. Bonferroni correction
422 was calculated with $\alpha = 0.05$.

423

424 **Relationship between worm genotype at chr. 2 and 3 and PZQ-R phenotype**

425 To validate the impact of worm genotypes on PZQ resistance phenotype and to determine whether PZQ-R
426 shows recessive, dominant or codominant inheritance, we measured the PZQ-R phenotype of individual
427 worms, and genotyped worms for markers at the peak of the QTLs located.

428

429 *Measuring PZQ-R in individual worms*

430 We plated 120 SmLE-PZQ-R adult male worms individually in 96-well plates, treated them with PZQ (24.3
431 $\mu\text{g}/\text{mL}$) and collected media supernatants pre- (24 h) and post- (48 h) treatment, and used L-lactate assays
432 to determine PZQ-R status. We extracted gDNA from each worm individually (66).

433

434 *PCR-RFLP for chr.2 and chr.3 loci*

435 We used PCR-RFLP to genotype single worms at loci marking QTL peaks on chr. 2 (C>A, chr SM_V7_2:
436 1072148) and chr. 3 (T>C, chr SM_V7_3: 741987) (Table S4). We digested PCR amplicons for chr. 2 with
437 BslI (NEB) and chr. 3 with MseI (NEB), and visualized digested PCR amplicons by 2% agarose gel
438 electrophoresis.

439

440 Quantitative PCR of copy number variation (CNV) in single worms

441 We genotyped individual worms for a deletion on chr. 3 (position 1220683-1220861 bp) using a qPCR
442 assay. Methods and primers are described in Table S4.

443

444 **Marker assisted selection of resistant and susceptible parasite populations**

445 Selection of SmLE-PZQ-ER and SmLE-PZQ-ES populations

446 We separated the polymorphic SmLE-PZQ-R schistosome population based on chr. 3 QTL genotype using
447 PCR-RFLP. We exposed 960 inbred *B. glabrata* Bg121 snails to one miracidium SmLE-PZQ-R (66). At
448 four weeks post-exposure, we identified infected snails ($N=272$), collected cercariae from individual snails,
449 extracted cercarial DNA (66), and genotyped each parasite for the chr. 3 locus using PCR-RFLP
450 (Homozygous R/R: $n=89 - 36\%$; Homozygous S/S: $n=39 - 16\%$; Heterozygous R/S: $n=117 - 49\%$), and
451 determined their gender by PCR (72). We selected 32 R/R parasites and 32 S/S genotypes. For both R/R
452 and S/S we used 13 males and 19 females. We exposed 5 hamsters to 800 cercariae of 32 R/R genotypes
453 parasites and 5 hamsters to 800 cercariae 32 S/S genotyped parasites. This single generation marker assisted
454 selection procedure generates two subpopulations: SmLE-PZQ-ER is enriched for parasites with R/R
455 genotype, while SmLE-PZQ-ES is enriched for S/S genotypes.

456

457 PZQ IC_{50} with SmLE-PZQ-ER and SmLE-PZQ-ES

458 Forty-five days after infection, we euthanized and perfused hamsters to recover adult schistosome worms
459 for SmLE-PZQ-ER and SmLE-PZQ-ES subpopulations. We placed adult males in 96-well plates and
460 cultured in 250 μ L DMEM complete media. We determined PZQ dose-response for both SmLE-PZQ-ER
461 and SmLE-PZQ-ES population.

462

463 gDNA extraction and library preparation and bioinformatics

464 We recovered the F1 SmLE-PZQ-ER and SmLE-PZQ-ES worms and extracted gDNA from pools of adult
465 males or females separately. We prepared whole genome libraries from these pools in triplicate using the

466 KAPA HyperPlus kit (KAPA Biosystems). Sequence data are available at the NCBI Sequence Read
467 Archive (accession numbers PRJNA701978). The analysis was identical to the GWAS and QTL mapping
468 analysis (see Jupyter notebook and scripts (https://github.com/fdchevalier/PZQ-R_DNA)).

469

470 **Transcriptomic analysis of resistant and susceptible schistosome worms at juvenile and adult stages**

471 Sample collection

472 We recovered *S. mansoni* SmLE-PZQ-ER and SmLE-PZQ-ES worms by perfusion from hamsters at 28
473 days (juveniles) or 45 days (adults) post-infection. For each subpopulation, (SmLE-PZQ-ER or SmLE-
474 PZQ-ES), we collected 3 biological replicates of 30 males or 30 females for the 28d juvenile worms, and 3
475 biological replicates of 30 males or 60 females for the 45d adult worms.

476

477 RNA extraction and RNAseq library preparation

478 ***a. RNA extraction***

479 We extracted total RNA from all the *S. mansoni* adult and juvenile worms (RNeasy Mini kit, Qiagen),
480 quantified the RNA recovered (Qubit RNA Assay Kit, Invitrogen) and assessed the RNA integrity by
481 TapeStation (Agilent - RNA integrity numbers: ~8.5–10 for all samples).

482 ***b. RNAseq library preparation***

483 We prepared RNAseq libraries using the KAPA Stranded mRNA-seq kit (KAPA Biosystems) using 500ng
484 RNA for each library. We sequenced the libraries using 150 bp pair-end reads. Raw sequence data are
485 available at the NCBI Sequence Read Archive (accession numbers PRJNA704646).

486 ***c. Bioinformatic analysis.***

487 To identify differentially expressed genes, we aligned the sequencing data against the *S. mansoni* reference
488 genome using STAR. We quantified gene and isoform abundances by computing transcripts per million
489 values using RSEM and compared abundances between groups (ES/ER, males/females, juveniles/adults)
490 using the R package EBSeq.

491

492 **Manipulation of *Sm.TRPM_{PZQ}* channel expression or function:**

493 **RNA interference**

494 We attempted RNA interference to functionally validate the implication of *Sm.TRPM_{PZQ}* on schistosome
495 PZQ resistance. The methods used are described in File S1 and Table S2, but were unsuccessful so are not
496 described here.

497

498 **Specific *Sm.TRPM_{PZQ}* chemical inhibitor and activators**

499 We used specific chemical inhibitor and activators (Chulkov *et al.*, in prep) to manipulate the function of
500 *Sm.TRPM_{PZQ}* to examine the impact on PZQ-response. We placed individual SmLE-PZQ-ER and SmLE-
501 PZQ-ES adult male worms in 96-well plates containing DMEM complete media. After 24h, 20 worms from
502 each population were treated either with a cocktail combining PZQ (1 µg/mL) and i) 50 µM of *Sm.TRPM_{PZQ}*
503 blocker (MB2) or ii) 10 µM, 25 µM or 50 µM of *Sm.TRPM_{PZQ}* activator (MV1) respectively or iii) drug
504 diluent (DMSO). We also set up control plates to evaluate the impact of *Sm.TRPM_{PZQ}* blocker or activator
505 alone. Worms were exposed to these drug cocktails for 24h, washed 3 times with drug-free medium, and
506 incubated (37°C, 5% CO₂) for 2 days. We collected media supernatants (125µL) before treatment (after 24h
507 in culture) and 48h post-treatment and quantified lactate levels.

508

509 **In vivo parasite survival after PZQ treatment**

510 We split 24 female Balb/C mice into two groups: one group exposed by tail immersion to SmLE-PZQ-ER
511 (80 cercariae/mouse from 40 infected snails) and the second one to SmLE-PZQ-ES (80 cercariae/mouse
512 from 40 infected snails). Forty days post-infection, we treated mice by oral gavage with either 120mg/kg
513 of PZQ (1% DMSO + vegetable oil in a total volume of 150 µL) or the same volume of drug diluent only
514 (control group). We euthanized and perfused (65) mice (day 50 post-infection) to recover worms.

515

516 ***Sm.TRPM_{PZQ}* variants in *S. mansoni* field samples**

517 *Variants identification in exome-sequenced data from natural S. mansoni parasites*

518 We utilized exome sequence data from *S. mansoni* from Africa, South America and the middle East to
519 investigate variation in *Sm.TRPM_{PZQ}*. African miracidia were from the Schistosomiasis collection at the
520 Natural History Museum (SCAN) (73), Brazilian miracidia and Omani cercariae and adult worms were
521 collected previously. We have previously described exome sequencing methods for *S. mansoni* (51, 52).
522 Data were analyzed the same way as described in Chevalier et al. (52). Code is available in Jupyter notebook
523 and scripts associated (https://github.com/fdchevalier/PZQ-R_field).

524

525 *Sanger re-sequencing to confirm the presence of the Sm.TRPM_{PZQ} field variants*

526 To confirm the presence of variants in *Sm.TRPM_{PZQ}* (when read depth was <10 reads), we performed Sanger
527 re-sequencing of mutations of interest close to the PZQ binding site (21). Primers and conditions are listed
528 in Table S4. We scored variants using PolyPhred software (v6.18) (Nickerson et al., 1997). Sequences are
529 deposited in GenBank (KU951903-KU952091).

530

531 **Statistical analysis**

532 Statistical analyzes and graphs were performed using R software (v3.5.1) (74). We used the drc package
533 from R to analyze dose-response datasets and Readqpcr and Normqpcr packages to analyze RT-qPCR
534 datasets. For non-normal data (Shapiro test, $p < 0.05$), we used Chi-square test, Kruskal-Wallis test followed
535 by pairwise Wilcoxon-Mann-Whitney post-hoc test or a Wilcoxon-Mann-Whitney test. For normal data,
536 we used one-way ANOVA or a pairwise comparison Welsh *t*-test. The confidence intervals were set to
537 95% and *p*-values < 0.05 were considered significant.

538

539 **Supplementary Materials**

540 Fig. S1. Development of a lactate assay for assaying worm recovery.

541 Fig. S2. Validation of marker-assisted selection of SmLE-PZQ-ER and ES using Next Generation
542 Sequencing (NGS).

543 Fig. S3. Large deletions adjacent to *Sm.TRPM_{PZQ}* and SOX13 transcription factor.

544 Fig. S4. Detailed genes and isoforms expression in SmLE-PZQ-ER and SmLE-PZQ-ES parasites.

545 Fig. S5. Cellular localization of *Sm.TRPM_{PZQ}* expression in *S. mansoni*.

546 Fig. S6. Impact of *in vivo* PZQ treatment on SmLE-PZQ-ER and SmLE-PZQ-ES parasites.

547 Fig. S7. Stop codon identified in *S. mansoni* field sample from Oman.

548 Table S1. Genes in QTL regions on chr. 2 and 3.

549 Table S2. Details of RNAi for *Sm.TRPM_{PZQ}*.

550 Table S3. Mutations present in *Sm.TRPM_{PZQ}* in natural schistosome populations from 3 African countries
551 (Senegal, Niger, Tanzania), the Middle East (Oman) and South America (Brazil).

552 Table S4. Summary table of siRNA sequences and primer sequences used for PCR-RFLP, RT-qPCR, PCRs
553 and Sanger sequencing.

554 File S1. Expanded Material and Methods.

555

556 **References and Notes**

- 557 1. World Health Organization, Schistosomiasis, (available at [https://www.who.int/news-room/fact-](https://www.who.int/news-room/fact-sheets/detail/schistosomiasis)
558 [sheets/detail/schistosomiasis](https://www.who.int/news-room/fact-sheets/detail/schistosomiasis)).
- 559 2. G. B. D. 2017 Disease, I. Incidence, P. Collaborators, Global, regional, and national incidence, prevalence, and
560 years lived with disability for 354 diseases and injuries for 195 countries and territories, 1990-2017: a systematic
561 analysis for the Global Burden of Disease Study 2017., *Lancet (London, England)* **392**, 1789–1858 (2018).
- 562 3. D. P. McManus, D. W. Dunne, M. Sacko, J. Utzinger, B. J. Vennervald, X.-N. Zhou, Schistosomiasis., *Nature*
563 *reviews. Disease primers* **4**, 13 (2018).
- 564 4. G. B. D. 2015 Mortality, C. of Death Collaborators, Global, regional, and national life expectancy, all-cause
565 mortality, and cause-specific mortality for 249 causes of death, 1980-2015: a systematic analysis for the Global
566 Burden of Disease Study 2015., *Lancet (London, England)* **388**, 1459–1544 (2016).
- 567 5. M. A. Verjee, Schistosomiasis: Still a cause of significant morbidity and mortality., *Research and reports in*
568 *tropical medicine* **10**, 153–163 (2019).
- 569 6. M. J. van der Werf, S. J. de Vlas, S. Brooker, C. W. N. Looman, N. J. D. Nagelkerke, J. D. F. Habbema, D.
570 Engels, Quantification of clinical morbidity associated with schistosome infection in sub-Saharan Africa., *Acta Trop*
571 **86**, 125–139 (2003).
- 572 7. W. H. Organization, others, Schistosomiasis: progress report 2001-2011, strategic plan 2012-2020, (2013).
- 573 8. A. K. Deol, F. M. Fleming, B. Calvo-Urbano, M. Walker, V. Bucumi, I. Gnadou, E. M. Tukahebwa, S. Jemu, U.
574 J. Mwingira, A. Alkohlani, M. Traoré, E. Ruberanziza, S. Touré, M.-G. Basáñez, M. D. French, J. P. Webster,
575 Schistosomiasis - assessing progress toward the 2020 and 2025 global goals., *The New England journal of medicine*
576 **381**, 2519–2528 (2019).
- 577 9. S. H. Xiao, P. A. Friedman, B. A. Catto, L. T. Webster, Praziquantel-induced vesicle formation in the tegument of
578 male *Schistosoma mansoni* is calcium dependent., *The Journal of parasitology* **70**, 177–179 (1984).
- 579 10. R. Pax, J. L. Bennett, R. Fetterer, A benzodiazepine derivative and praziquantel: effects on musculature of
580 *Schistosoma mansoni* and *Schistosoma japonicum*., *Naunyn-Schmiedeberg's archives of pharmacology* **304**, 309–
581 315 (1978).
- 582 11. B. Becker, H. Mehlhorn, P. Andrews, H. Thomas, J. Eckert, Light and electron microscopic studies on the effect
583 of praziquantel on *Schistosoma mansoni*, *Dicrocoelium dendriticum*, and *Fasciola hepatica* (Trematoda) in vitro.,
584 *Zeitschrift fur Parasitenkunde (Berlin, Germany)* **63**, 113–128 (1980).
- 585 12. C. S. Bricker, J. W. Deppenbusch, J. L. Bennett, D. P. Thompson, The relationship between tegumental disruption
586 and muscle contraction in *Schistosoma mansoni* exposed to various compounds., *Zeitschrift fur Parasitenkunde*
587 *(Berlin, Germany)* **69**, 61–71 (1983).
- 588 13. P. M. Cupit, C. Cunningham, What is the mechanism of action of praziquantel and how might resistance strike?,
589 *Future medicinal chemistry* **7**, 701–705 (2015).
- 590 14. C. M. Thomas, D. J. Timson, The mechanism of action of praziquantel: Six hypotheses., *Current topics in*
591 *medicinal chemistry* **18**, 1575–1584 (2018).
- 592 15. A. B. Kohn, P. A. Anderson, J. M. Roberts-Misterly, R. M. Greenberg, Schistosome calcium channel beta
593 subunits. Unusual modulatory effects and potential role in the action of the antischistosomal drug praziquantel., *The*
594 *Journal of biological chemistry* **276**, 36873–36876 (2001).

- 595 16. M. C. Jeziorski, R. M. Greenberg, Voltage-gated calcium channel subunits from platyhelminths: potential role in
596 praziquantel action., *International journal for parasitology* **36**, 625–632 (2006).
- 597 17. J. D. Chan, M. Zarowiecki, J. S. Marchant, Ca²⁺ channels and praziquantel: a view from the free world.,
598 *Parasitology international* **62**, 619–628 (2013).
- 599 18. R. S. Kasinathan, L. K. Sharma, C. Cunningham, T. R. Webb, R. M. Greenberg, Inhibition or knockdown of
600 ABC transporters enhances susceptibility of adult and juvenile schistosomes to Praziquantel., *PLoS neglected*
601 *tropical diseases* **8**, e3265 (2014).
- 602 19. R. M. Greenberg, ABC multidrug transporters in schistosomes and other parasitic flatworms., *Parasitology*
603 *international* **62**, 647–653 (2013).
- 604 20. S.-K. Park, G. S. Gunaratne, E. G. Chulkov, F. Moehring, P. McCusker, P. I. Dosa, J. D. Chan, C. L. Stucky, J.
605 S. Marchant, The anthelmintic drug praziquantel activates a schistosome transient receptor potential channel., *The*
606 *Journal of biological chemistry* **294**, 18873–18880 (2019).
- 607 21. S.-K. Park, L. Friedrich, N. A. Yahya, C. Rohr, E. G. Chulkov, D. Maillard, F. Rippmann, T. Spangenberg, J. S.
608 Marchant, Mechanism of praziquantel action at a parasitic flatworm ion channel, *bioRxiv* (2021),
609 doi:10.1101/2021.03.09.434291.
- 610 22. P. G. Fallon, M. J. Doenhoff, Drug-resistant schistosomiasis: resistance to praziquantel and oxamniquine
611 induced in *Schistosoma mansoni* in mice is drug specific., *Am J Trop Med Hyg* **51**, 83–88 (1994).
- 612 23. B. Gryseels, L. Nkulikyinka, D. Engels, Impact of repeated community-based selective chemotherapy on
613 morbidity due to schistosomiasis mansoni., *The American journal of tropical medicine and hygiene* **51**, 634–641
614 (1994).
- 615 24. M. Ismail, S. Botros, A. Metwally, S. William, A. Farghally, L. F. Tao, T. A. Day, J. L. Bennett, Resistance to
616 praziquantel: direct evidence from *Schistosoma mansoni* isolated from Egyptian villagers., *The American journal of*
617 *tropical medicine and hygiene* **60**, 932–935 (1999).
- 618 25. D. Alonso, J. Muñoz, J. Gascón, M. E. Valls, M. Corachan, Failure of standard treatment with praziquantel in
619 two returned travelers with *Schistosoma haematobium* infection., *The American journal of tropical medicine and*
620 *hygiene* **74**, 342–344 (2006).
- 621 26. F. F. B. Couto, P. M. Z. Coelho, N. Araújo, J. R. Kusel, N. Katz, L. K. Jannotti-Passos, A. C. A. Mattos,
622 *Schistosoma mansoni*: a method for inducing resistance to praziquantel using infected *Biomphalaria glabrata* snails.,
623 *Memorias do Instituto Oswaldo Cruz* **106**, 153–157 (2011).
- 624 27. W. Wang, L. Wang, Y.-S. Liang, Susceptibility or resistance of praziquantel in human schistosomiasis: a
625 review., *Parasitology research* **111**, 1871–1877 (2012).
- 626 28. D. Cioli, S. S. Botros, K. Wheatcroft-Francklow, A. Mbaye, V. Southgate, L.-A. T. Tchuenté, L. Pica-Mattoccia,
627 A. R. Troiani, S. H. S. El-Din, A.-N. A. Sabra, J. Albin, D. Engels, M. J. Doenhoff, Determination of ED50 values
628 for praziquantel in praziquantel-resistant and -susceptible *Schistosoma mansoni* isolates., *International journal for*
629 *parasitology* **34**, 979–987 (2004).
- 630 29. L. Pica-Mattoccia, M. J. Doenhoff, C. Valle, A. Basso, A.-R. Troiani, P. Liberti, A. Festucci, A. Guidi, D. Cioli,
631 Genetic analysis of decreased praziquantel sensitivity in a laboratory strain of *Schistosoma mansoni*., *Acta Trop* **111**,
632 82–85 (2009).
- 633 30. J. Zwang, P. Olliaro, Efficacy and safety of praziquantel 40 mg/kg in preschool-aged and school-aged children: a
634 meta-analysis., *Parasites & vectors* **10**, 47 (2017).

- 635 31. L. Pica-Mattocchia, D. Cioli, Sex- and stage-related sensitivity of *Schistosoma mansoni* to in vivo and in vitro
636 praziquantel treatment., *International journal for parasitology* **34**, 527–533 (2004).
- 637 32. S. Botros, L. Pica-Mattocchia, S. William, N. El-Lakkani, D. Cioli, Effect of praziquantel on the immature stages
638 of *Schistosoma haematobium*., *International journal for parasitology* **35**, 1453–1457 (2005).
- 639 33. M. Ismail, A. Metwally, A. Farghaly, J. Bruce, L. F. Tao, J. L. Bennett, Characterization of isolates of
640 *Schistosoma mansoni* from Egyptian villagers that tolerate high doses of praziquantel., *The American journal of*
641 *tropical medicine and hygiene* **55**, 214–218 (1996).
- 642 34. S. D. Melman, M. L. Steinauer, C. Cunningham, L. S. Kubatko, I. N. Mwangi, N. B. Wynn, M. W. Mutuku, D.
643 M. S. Karanja, D. G. Colley, C. L. Black, W. E. Secor, G. M. Mkoji, E. S. Loker, Reduced susceptibility to
644 praziquantel among naturally occurring Kenyan isolates of *Schistosoma mansoni*., *PLoS neglected tropical diseases*
645 **3**, e504 (2009).
- 646 35. S. William, S. Botros, M. Ismail, A. Farghally, T. A. Day, J. L. Bennett, Praziquantel-induced tegumental
647 damage in vitro is diminished in schistosomes derived from praziquantel-resistant infections., *Parasitology* **122 Pt 1**,
648 63–66 (2001).
- 649 36. N. Kittur, C. H. Campbell, S. Binder, Y. Shen, R. E. Wiegand, J. R. Mwangi, S. M. Kinung'hi, R. M. Musuva,
650 M. R. Odiere, S. H. Matendechero, S. Knopp, D. G. Colley, Discovering, defining, and summarizing persistent
651 hotspots in SCORE studies., *The American journal of tropical medicine and hygiene* **103**, 24–29 (2020).
- 652 37. P. A. Mawa, J. Kincaid-Smith, E. M. Tukahebwa, J. P. Webster, S. Wilson, Schistosomiasis morbidity hotspots:
653 Roles of the human host, the parasite and their interface in the development of severe morbidity., *Frontiers in*
654 *immunology* **12**, 635869 (2021).
- 655 38. T. Crellen, M. Walker, P. H. L. Lamberton, N. B. Kabatereine, E. M. Tukahebwa, J. A. Cotton, J. P. Webster,
656 Reduced efficacy of praziquantel against *Schistosoma mansoni* is associated with multiple rounds of mass drug
657 administration., *Clinical infectious diseases : an official publication of the Infectious Diseases Society of America*
658 **63**, 1151–1159 (2016).
- 659 39. A. V. Protasio, I. J. Tsai, A. Babbage, S. Nichol, M. Hunt, M. A. Aslett, N. De Silva, G. S. Velarde, T. J. C.
660 Anderson, R. C. Clark, C. Davidson, G. P. Dillon, N. E. Holroyd, P. T. LoVerde, C. Lloyd, J. McQuillan, G.
661 Oliveira, T. D. Otto, S. J. Parker-Manuel, M. A. Quail, R. A. Wilson, A. Zerlotini, D. W. Dunne, M. Berriman, A
662 systematically improved high quality genome and transcriptome of the human blood fluke *Schistosoma mansoni*.,
663 *PLoS Negl Trop Dis* **6**, e1455 (2012).
- 664 40. T. J. C. Anderson, P. T. LoVerde, W. Le Clec'h, F. D. Chevalier, Genetic crosses and linkage mapping in
665 schistosome parasites., *Trends Parasitol* **34**, 982–996 (2018).
- 666 41. S. K. Volkman, J. Herman, A. K. Lukens, D. L. Hartl, Genome-wide association studies of drug-resistance
667 determinants., *Trends in parasitology* **33**, 214–230 (2017).
- 668 42. J. Wit, C. M. Dilks, E. C. Andersen, Complementary approaches with free-living and parasitic nematodes to
669 understanding anthelmintic resistance., *Trends in parasitology* **37**, 240–250 (2021).
- 670 43. R. H. Fetterer, R. A. Pax, J. L. Bennett, Praziquantel, potassium and 2,4-dinitrophenol: analysis of their action
671 on the musculature of *Schistosoma mansoni*., *European journal of pharmacology* **64**, 31–38 (1980).
- 672 44. S. Howe, D. Zöphel, H. Subbaraman, C. Unger, J. Held, T. Engleitner, W. H. Hoffmann, A. Kreidenweiss,
673 Lactate as a novel quantitative measure of viability in *Schistosoma mansoni* drug sensitivity assays., *Antimicrobial*
674 *agents and chemotherapy* **59**, 1193–1199 (2015).

- 675 45. M. Girardot, E. Bayet, J. Maurin, P. Fort, P. Roux, P. Raynaud, SOX9 has distinct regulatory roles in alternative
676 splicing and transcription., *Nucleic acids research* **46**, 9106–9118 (2018).
- 677 46. G. Wendt, L. Zhao, R. Chen, C. Liu, A. J. O’Donoghue, C. R. Caffrey, M. L. Reese, J. J. Collins, A single-cell
678 RNA-seq atlas of , javax.xml.bind.JAXBElement@463bbb2c, identifies a key regulator of blood feeding., *Science*
679 (*New York, N.Y.*) **369**, 1644–1649 (2020).
- 680 47. S. William, A. Sabra, F. Ramzy, M. Mousa, Z. Demerdash, J. L. Bennett, T. A. Day, S. Botros, Stability and
681 reproductive fitness of *Schistosoma mansoni* isolates with decreased sensitivity to praziquantel., *International*
682 *journal for parasitology* **31**, 1093–1100 (2001).
- 683 48. S. Hernando-Amado, F. Sanz-García, P. Blanco, J. L. Martínez, Fitness costs associated with the acquisition of
684 antibiotic resistance., *Essays in biochemistry* **61**, 37–48 (2017).
- 685 49. P. Durão, R. Balbontín, I. Gordo, Evolutionary mechanisms shaping the maintenance of antibiotic resistance.,
686 *Trends in microbiology* **26**, 677–691 (2018).
- 687 50. S. Nair, X. Li, G. A. Arya, M. McDew-White, M. Ferrari, F. Nosten, T. J. C. Anderson, Fitness costs and the
688 rapid spread of , javax.xml.bind.JAXBElement@527e161e, -C580Y substitutions conferring artemisinin resistance.,
689 *Antimicrobial agents and chemotherapy* **62** (2018), doi:10.1128/AAC.00605-18.
- 690 51. W. Le Clec’h, F. D. Chevalier, M. McDew-White, F. Allan, B. L. Webster, A. N. Gouvras, S. Kinunghi, L.-A.
691 Tchuem Tchuenté, A. Garba, K. A. Mohammed, S. M. Ame, J. P. Webster, D. Rollinson, A. M. Emery, T. J. C.
692 Anderson, Whole genome amplification and exome sequencing of archived schistosome miracidia., *Parasitology*
693 **145**, 1739–1747 (2018).
- 694 52. F. D. Chevalier, W. Le Clec’h, M. McDew-White, V. Menon, M. A. Guzman, S. P. Holloway, X. Cao, A. B.
695 Taylor, S. Kinung’hi, A. N. Gouvras, B. L. Webster, J. P. Webster, A. M. Emery, D. Rollinson, A. Garba Djirmay,
696 K. M. Al Mashikhi, S. Al Yafae, M. A. Idris, H. Moné, G. Mouahid, P. J. Hart, P. T. LoVerde, T. J. C. Anderson,
697 Oxamniquine resistance alleles are widespread in Old World *Schistosoma mansoni* and predate drug deployment.,
698 *PLoS pathogens* **15**, e1007881 (2019).
- 699 53. D. Ménard, N. Khim, J. Beghain, A. A. Adegnika, M. Shafiul-Alam, O. Amodu, G. Rahim-Awab, C. Barnadas,
700 A. Berry, Y. Boum, M. D. Bustos, J. Cao, J.-H. Chen, L. Collet, L. Cui, G.-D. Thakur, A. Dieye, D. Djallé, M. A.
701 Dorkenoo, C. E. Eboumbou-Moukoko, F.-E.-C. J. Espino, T. Fandeur, M.-F. Ferreira-da-Cruz, A. A. Fola, H.-P.
702 Fuehrer, A. M. Hassan, S. Herrera, B. Hongvanthong, S. Houzé, M. L. Ibrahim, M. Jahirul-Karim, L. Jiang, S.
703 Kano, W. Ali-Khan, M. Khanthavong, P. G. Kremsner, M. Lacerda, R. Leang, M. Leelawong, M. Li, K. Lin, J.-B.
704 Mazarati, S. Ménard, I. Morlais, H. Muhindo-Mavoko, L. Musset, K. Na-Bangchang, M. Nambozi, K. Niaré, H.
705 Noedl, J.-B. Ouédraogo, D. R. Pillai, B. Pradines, B. Quang-Phuc, M. Ramharter, M. Randrianariveolosia, J.
706 Sattabongkot, A. Sheikh-Omar, K. D. Silué, S. B. Sirima, C. Sutherland, D. Syafruddin, R. Tahar, L.-H. Tang, O. A.
707 Touré, P. Tshibangu-wa-Tshibangu, I. Vigan-Womas, M. Warsame, L. Wini, S. Zakeri, S. Kim, R. Eam, L. Berne,
708 C. Khean, S. Chy, M. Ken, K. Loch, L. Canier, V. Duru, E. Legrand, J.-C. Barale, B. Stokes, J. Straimer, B.
709 Witkowski, D. A. Fidock, C. Rogier, P. Ringwald, F. Ariey, O. Mercereau-Puijalon, K. A. R. M. A. Consortium, A
710 worldwide map of plasmodium falciparum k13-propeller polymorphisms., *The New England journal of medicine*
711 **374**, 2453–2464 (2016).
- 712 54. M. Mayxay, S. Nair, D. Sudimack, M. Imwong, N. Tanomsing, T. Pongvongsa, S. Phompida, R. Phetsouvanh,
713 N. J. White, T. J. C. Anderson, P. N. Newton, Combined molecular and clinical assessment of Plasmodium
714 falciparum antimalarial drug resistance in the Lao People’s Democratic Republic (Laos)., *The American journal of*
715 *tropical medicine and hygiene* **77**, 36–43 (2007).
- 716 55. T. O. Apinjoh, A. Ouattara, V. P. K. Titanji, A. Djimde, A. Amambua-Ngwa, Genetic diversity and drug
717 resistance surveillance of Plasmodium falciparum for malaria elimination: is there an ideal tool for resource-limited
718 sub-Saharan Africa?, *Malaria journal* **18**, 217 (2019).

- 719 56. A. C. Kotze, R. K. Prichard, Anthelmintic resistance in haemonchus contortus: History, mechanisms and
720 diagnosis., *Advances in parasitology* **93**, 397–428 (2016).
- 721 57. L. A. Melville, E. Redman, A. A. Morrison, P. C. Rebecca Chen, R. Avramenko, S. Mitchell, J. Van Dijk, G.
722 Innocent, F. Sargison, C. Aitken, J. S. Gilleard, D. J. Bartley, Large scale screening for benzimidazole resistance
723 mutations in *Nematodirus battus*, using both pyrosequence genotyping and deep amplicon sequencing, indicates the
724 early emergence of resistance on UK sheep farms., *International journal for parasitology. Drugs and drug*
725 *resistance* **12**, 68–76 (2020).
- 726 58. C. L. L. Valentim, D. Cioli, F. D. Chevalier, X. Cao, A. B. Taylor, S. P. Holloway, L. Pica-Mattocchia, A. Guidi,
727 A. Basso, I. J. Tsai, M. Berriman, C. Carvalho-Queiroz, M. Almeida, H. Aguilar, D. E. Frantz, P. J. Hart, P. T.
728 LoVerde, T. J. C. Anderson, Genetic and molecular basis of drug resistance and species-specific drug action in
729 schistosome parasites., *Science (New York, N.Y.)* **342**, 1385–1389 (2013).
- 730 59. F. D. Chevalier, W. Le Clec'h, N. Eng, A. R. Rugel, R. R. de Assis, G. Oliveira, S. P. Holloway, X. Cao, P. J.
731 Hart, P. T. LoVerde, T. J. C. Anderson, Independent origins of loss-of-function mutations conferring oxamniquine
732 resistance in a Brazilian schistosome population., *International journal for parasitology* **46**, 417–424 (2016).
- 733 60. G. Mouahid, M. A. Idris, O. Verneau, A. Théron, M. M. A. Shaban, H. Moné, A new chronotype of
734 *Schistosoma mansoni*: adaptive significance., *Trop Med Int Health* **17**, 727–732 (2012).
- 735 61. R. K. Assaré, R. N. N'Tamon, L. G. Bellai, J. A. Koffi, T.-B. I. Mathieu, M. Ouattara, E. Hürlimann, J. T.
736 Coulibaly, S. Diabaté, E. K. N'Goran, J. Utzinger, Characteristics of persistent hotspots of *Schistosoma mansoni* in
737 western Côte d'Ivoire., *Parasites & vectors* **13**, 337 (2020).
- 738 62. K. M. Bonner, C. J. Bayne, M. K. Larson, M. S. Blouin, Effects of Cu/Zn superoxide dismutase (SOD1)
739 genotype and genetic background on growth, reproduction and defense in *Biomphalaria glabrata*., *PLoS Negl Trop*
740 *Dis* **6**, e1701 (2012).
- 741 63. F. A. Lewis, M. A. Stirewalt, C. P. Souza, G. Gazzinelli, Large-scale laboratory maintenance of *Schistosoma*
742 *mansoni*, with observations on three schistosome/snail host combinations., *J Parasitol* **72**, 813–829 (1986).
- 743 64. D. Cioli, L. Pica-Mattocchia, R. Moroni, *Schistosoma mansoni*: hycanthone/oxamniquine resistance is controlled
744 by a single autosomal recessive gene., *Experimental parasitology* **75**, 425–432 (1992).
- 745 65. R. H. Duvall, W. B. DeWitt, An improved perfusion technique for recovering adult schistosomes from
746 laboratory animals., *The American journal of tropical medicine and hygiene* **16**, 483–486 (1967).
- 747 66. W. Le Clec'h, R. Diaz, F. D. Chevalier, M. McDew-White, T. J. C. Anderson, Striking differences in virulence,
748 transmission and sporocyst growth dynamics between two schistosome populations., *Parasites & vectors* **12**, 485
749 (2019).
- 750 67. H. Li, R. Durbin, Fast and accurate short read alignment with Burrows-Wheeler transform., *Bioinformatics*
751 *(Oxford, England)* **25**, 1754–1760 (2009).
- 752 68. H. Li, B. Handsaker, A. Wysoker, T. Fennell, J. Ruan, N. Homer, G. Marth, G. Abecasis, R. Durbin, 1000
753 Genome Project Data Processing Subgroup, The sequence Alignment/Map format and SAMtools., *Bioinformatics*
754 *(Oxford, England)* **25**, 2078–2079 (2009).
- 755 69. M. A. DePristo, E. Banks, R. Poplin, K. V. Garimella, J. R. Maguire, C. Hartl, A. A. Philippakis, G. del Angel,
756 M. A. Rivas, M. Hanna, A. McKenna, T. J. Fennell, A. M. Kernysky, A. Y. Sivachenko, K. Cibulskis, S. B.
757 Gabriel, D. Altshuler, M. J. Daly, A framework for variation discovery and genotyping using next-generation DNA
758 sequencing data., *Nature genetics* **43**, 491–498 (2011).

- 759 70. A. McKenna, M. Hanna, E. Banks, A. Sivachenko, K. Cibulskis, A. Kernytsky, K. Garimella, D. Altshuler, S.
760 Gabriel, M. Daly, M. A. DePristo, The genome analysis toolkit: a MapReduce framework for analyzing next-
761 generation DNA sequencing data., *Genome research* **20**, 1297–1303 (2010).
- 762 71. J. Köster, S. Rahmann, Snakemake—a scalable bioinformatics workflow engine., *Bioinformatics (Oxford,*
763 *England)* **34**, 3600 (2018).
- 764 72. F. D. Chevalier, W. Le Clec'h, A. C. Alves de Mattos, P. T. LoVerde, T. J. C. Anderson, Real-time PCR for
765 sexing *Schistosoma mansoni* cercariae., *Mol Biochem Parasitol* **205**, 35–38 (2016).
- 766 73. A. M. Emery, F. E. Allan, M. E. Rabone, D. Rollinson, Schistosomiasis collection at NHM (SCAN)., *Parasites*
767 *& vectors* **5**, 185 (2012).
- 768 74. R Core Team, R: A language and environment for statistical computing, *R Foundation for Statistical Computing*
769 *- Vienna, Austria* (2018).
- 770 75. M. O.J., PerlPrimer: cross-platform, graphical primer design for standard, bisulphite and real-time PCR.,
771 *Bioinformatics* **20**, 2471–2 (2004).
- 772 76. G. Krautz-Peterson, R. Bhardwaj, Z. Faghiri, C. A. Tararam, P. J. Skelly, RNA interference in schistosomes:
773 machinery and methodology., *Parasitology* **137**, 485–495 (2010).
- 774 77. R. Bhardwaj, G. Krautz-Peterson, P. J. Skelly, Using RNA interference in schistosoma mansoni., *Methods in*
775 *molecular biology (Clifton, N.J.)* **764**, 223–239 (2011).
- 776 78. X. Rao, X. Huang, Z. Zhou, X. Lin, An improvement of the 2⁻(-delta delta CT) method for quantitative real-time
777 polymerase chain reaction data analysis., *Biostatistics, bioinformatics and biomathematics* **3**, 71–85 (2013).
- 778 79. G. Krautz-Peterson, R. Bhardwaj, Z. Faghiri, C. A. Tararam, P. J. Skelly, RNA interference in schistosomes:
779 machinery and methodology., *Parasitology* **137**, 485–495 (2010).
- 780 80. W. Le Clec'h, R. Diaz, F. D. Chevalier, M. McDew-White, T. J. C. Anderson, Striking differences in virulence,
781 transmission and sporocyst growth dynamics between two schistosome populations., *Parasites & vectors* **12**, 485
782 (2019).

783

784 **Acknowledgments:** We thank the Vivarium of the Southwest National Primate Research Center (SNPRC)
785 for providing rodent care. This research was supported by a Cowles fellowship (WLC) from Texas
786 Biomedical Research Institute (13-1328.021), and NIH R01AI133749 (TJCA) and was conducted in
787 facilities constructed with support from Research Facilities Improvement Program grant C06 RR013556
788 from the National Center for Research Resources. SNPRC research at Texas Biomedical Research Institute
789 is supported by grant P51 OD011133 from the 570 Office of Research Infrastructure Programs, NIH.
790 Miracidia samples for sequence analysis were provided by Schistosomiasis Collection at the Natural
791 History Museum (SCAN) funded by the Wellcome Trust (grant 104958/Z/14/Z) and curated Muriel

792 Rabone. We thank Dr Oumar T. Diaw and Moumoudane M. Seye (Institut Sénégalais de Recherches
793 Agricoles, Senegal) for the collections in Senegal (EU-CONTRAST project); Dr Anouk Gouvras (Global
794 Schistosomiasis Alliance (GSA)), Mariama Lamine and the Réseau International Schistosomiasis
795 Environnemental Aménagement et Lutte (RISEAL) team (Niger) for the collections in Niger; Dr Anouk
796 Gouvras (GSA) and the National Institute for Medical Research (NIMR, Mwanza Tanzania) team Dr Teckla
797 Angelo, Honest Nagai, Boniface Emmanuel, John Igogote, Sarah Buddenborg and Reuben Jonathan for the
798 collections in Tanzania as part of the Schistosomiasis Consortium for Operational Research and Evaluation
799 (SCORE) project (<https://score.uga.edu>).

800 **Funding:**

801 National Institutes of Health grant [1R01AI123434](#) (TJCA, PTL)
802 National Institutes of Health grant 1R01AI133749 (TJCA)
803 National Institutes of Health grant NIH R01AI145871 (JSM)
804 Ministry of Health in Oman, the Sultan Qaboos University (grant no. IG/ MED/MICR/00/01)
805 French Ministry of Foreign Affairs (French Embassy in Oman) (grants nos. 402419B, 402415K
806 and 339660F)
807 CNRS- Sciences de la Vie (grants no. 01N92/0745/1 and 02N60/1340)
808 CNRS-Direction des Relations internationales (grants no. 01N92/0745 and 02N60/1340)
809 PICS-CNRS no. 06249: FRANC-INCENSE

810 **Author contributions:**

811 Conceptualization: WLC, PTL, TJCA
812 Methodology: WLC, FDC, PTL, JM
813 Investigation: WLC, FDC, ACM, AS, RD, JM
814 Visualization: WLC, FDC
815 Field samples: HM, GM, MI, KAM, SAY
816 Funding acquisition: TJCA, PTL, JM, HM, GM

817 Project administration: TJCA, PTL
818 Supervision: TJCA, WLC, FDC, PTL, JM
819 Writing – original draft: TJCA, WLC, FDC
820 Writing – review & editing: TJCA, WLC, FDC, PTL, JM, HM, GM

821 **Competing interests:** Authors declare that they have no competing interests.

822 **Data and materials availability:**

823 Sequence data is available from: PRJNA699326, PRJNA701978, PRJNA704646

824 Sequence data from field collected *S. mansoni* is available from: PRJNA439266, PRJNA560070,
825 PRJNA560069, PRJNAXXXXXX

826 Code is available from: https://github.com/fdchevalier/PZQ-R_DNA, https://github.com/fdchevalier/PZQ-R_RNA, https://github.com/fdchevalier/PZQ-R_field

828

829 **File S1.**

830 **EXPANDED MATERIALS AND METHODS**

831 **Study design**

832 This study was designed to determine the genetic basis of PZQ-R, and was stimulated by the initial
833 observation that a laboratory *S. mansoni* population generated through selection with PZQ contained both
834 PZQ-S and PZQ-R individuals. The project had 6 stages: (i) QTL location. We conducted a genome-wide
835 association study (GWAS). This involved measuring the PZQ-response of individual worms, pooling those
836 showing high levels of resistance and low levels of resistance, sequencing the pools to high read depth, and
837 then identifying the genome regions showing significant differences in allele frequencies between high and
838 low resistance parasites. (ii) Fine mapping of candidate genes. We identified potential candidate genes in
839 these QTL regions, through examination of gene annotations, and exclusion of genes that are not expressed
840 in adults. We also determined whether the loci determining PZQ-R are inherited in a recessive, dominant
841 or co-dominant manner (iii) Marker assisted purification of PZQ-S and PZQ-R parasites. To separate PZQ-
842 R and PZQ-S parasites into “pure” populations, we genotyped larval parasites for genetic markers in the
843 QTL regions and infected rodents with genotypes associated with PZQ-R or PZQ-S. To verify that this
844 approach worked, we then measured the IC₅₀ for each of the purified populations. (iv) Characterization of
845 purified SmLE-PZQ-ER and SmLE-PZQ-ES populations. Separation of SmLE-PZQ-ES and SmLE-PZQ-
846 ER parasite populations allowed us to characterize these in more detail. Specifically, we measured
847 expression in juvenile and adult worms of both sexes in both SmLE-PZQ-ES and SmLE-PZQ-ER parasites.
848 We also quantified parasite fitness traits. (v) Functional analysis. We used RNAi and chemical manipulation
849 approaches to modulate activity of candidate genes and determine the impact of PZQ-resistance. We also
850 used transient expression of candidate genes in cultured mammalian cells, to determine the impact of
851 particular SNPs on response to PZQ-exposure. (vi) Survey of PZQ-resistance variants in field collected
852 parasites. Having determined the gene underlying PZQ-R in laboratory parasites, we examined sequence

853 variation in this gene in a field collection of *S. mansoni* parasites collected to examine the frequency of
854 sequence variants predicted to result in PZQ-resistance.

855

856 Ethics statement

857 This study was performed in accordance with the Guide for the Care and Use of Laboratory Animals of the
858 National Institutes of Health. The protocol was approved by the Institutional Animal Care and Use
859 Committee of Texas Biomedical Research Institute (permit number: 1419-MA and 1420-MU). Details of
860 ethical permission for collection of samples from humans are described in Chevalier et al. (51, 52).

861

862 **Biomphalaria glabrata snails and Schistosoma mansoni parasites**

863 Uninfected inbred albino *Biomphalaria glabrata* snails (line Bg121 derived from 13-16-R1 line (62)) were
864 reared in 10-gallon aquaria containing aerated freshwater at 26-28 °C on a 12L-12D photcycle and fed *ad*
865 *libitum* on green leaf lettuce. All snails used in this study had a shell diameter between 8 and 10 mm. We
866 used inbred snails to minimize the impact of snail host genetic background on the parasite life history traits
867 (66).

868 The SmLE schistosome (*Schistosoma mansoni*) population was originally obtained from an
869 infected patient in Belo Horizonte (Minas Gerais, Brazil) in 1965 and has since been maintained in
870 laboratory (63), using *B. glabrata* NMRI, inbred Bg36 and Bg121 population as intermediate snail host and
871 Syrian golden hamsters (*Mesocricetus auratus*) as definitive hosts. The SmLE-PZQ-R schistosome
872 population was generated in Brazil by applying a single round of PZQ selection pressure on SmLE parasites
873 at both snail and rodent stages (26). The SmLE-PZQ-R population has been maintained in our laboratory
874 using *B. glabrata* NMRI, Bg36 and Bg121 snail population and hamsters as the definitive host since 2014.

875

876 **Drug resistance tests:**

877 *Dose-response curves to PZQ in SmLE and SmLE-PZQ-R populations*

878 Drug sensitivity to Praziquantel (PZQ) was initially measured using a modified protocol (64) in SmLE and
879 SmLE-PZQ-R parasite populations. Ten adult males, recovered by perfusion from infected hamsters (t+ 45
880 days post-infection) (65) from SmLE or SmLE-PZQ-R population were placed into each well of a 24-well
881 microplate containing 1 mL of High glucose DMEM supplemented with 15% heat-inactivated fetal bovine
882 serum, 100 U/mL penicillin and 100µg/mL streptomycin (DMEM complete media). We performed control
883 and experimental groups in triplicate (N=240 worms/parasite populations). We exposed adult worms to
884 PZQ (0.1 µg/mL, 0.3 µg/mL, 0.9 µg/mL, 2.7 µg/mL, 8.1 µg/mL, 24.3 µg/mL and 72.9 µg/mL) for 24h.
885 Worms were then washed three times in drug-free medium and incubated (37°C, 5% CO₂) for 2 days.
886 Control groups were exposed only to the drug diluent dimethyl sulfoxide (DMSO). The parasites were
887 observed daily under a stereomicroscope for the 5 days of the experiment and the number of dead worms
888 visually scored. Worms were defined as “dead” if they showed no movements and became opaque. We
889 scored PZQ-resistance as a binary trait: parasites that recovered were classed as resistant, while parasites
890 that failed to recover were classed as sensitive.

891

892 Metabolic assessment of worm viability using L-lactate assay

893 We adapted a method for metabolic assessment of worm viability using L-lactate assay (44). Briefly, adult
894 male SmLE-PZQ-R worms recovered from infected hamsters were placed individually in 96-well plates
895 containing 100 µm mesh filter insert (Millipore) in 250µL DMEM complete media, and allowed to adapt
896 for 24 h. We added PZQ (24.3 µg/mL in DMEM complete media) for the PZQ treated group, while controls
897 were treated with the same volume of drug diluent DMSO. We also added a heat-killed worm control group:
898 adult male worms were placed into a microfuge tube containing distilled water and heated in a dry bath
899 (80°C, 15 min), and then plated in 96-well plate with 100 µm mesh insert. Drug resistance test was
900 conducted as described above (see *Dose-response curves to PZQ in SmLE and SmLE-PZQ-R populations*).
901 At 48h post-treatment, the supernatant (125 µL) was collected from each well and immediately stored at -
902 80 °C until processing.

903 We measured lactate levels in the supernatants of *in vitro* treated adult male worms with a
904 colorimetric L-lactate assay kit (Sigma) using 96-well, optical clear-bottom plates (Corning) following the
905 manufacturer's specifications, with minor modifications. Briefly, 5 μ L of supernatant were diluted into 20
906 μ L of ddH₂O to fit within the linear range of the assay. We then combine 24 μ L of the assay buffer to 1 μ L
907 of diluted supernatant (1/5 dilution) in each test well. and added 25 μ L of the lactate reaction mix (24 μ L
908 of the assay buffer, 0.5 μ L of enzyme mix and 0.5 μ L of lactate assay probe - $V_{\text{total}}= 50 \mu\text{L}/\text{well}$). We also
909 made a lactate standard curve to allow accurate lactate quantification in worm supernatants. After 45 min
910 of incubation in the dark at room temperature, the plate was read by a spectrophotometer (Molecular
911 Devices) at 570 nm. Lactate quantities in worm supernatant were assessed following the manufacturer's
912 instruction, taking in account our dilution factor. All measurement series included a DMEM complete
913 media control to determine the background lactate level, which was then subtracted from the lactate quantity
914 of the respective measurements.

915

916 **Genome wide association analysis and QTL mapping**

917 Schistosome infections

918 Eggs were collected from livers of hamster infected with SmLE-PZQ-R and hatched under light for 30 min
919 in freshwater to obtain miracidia (66). We then exposed one thousand Bg121 snails to five miracidia/snail.
920 After 30 days, snails were individually exposed to light in 24-well plates to shed cercariae. Eight hamsters
921 were exposed to 840 cercariae (4 cercariae/snail) from a batch of 210 shedding snails. We euthanized
922 hamsters after 45 days to collect adult worms.

923

924 Phenotypic selection

925 Adult SmLE-PZQ-R worms were collected, separated by sex and males were plated individually in 96-well
926 plates (60 worms per plate) containing 100 μ M mesh filter insert (Millipore) in 250 μ L of DMEM complete
927 media and treated with a dose of 24.3 μ g/mL PZQ as describe above (i.e. *Metabolic assessment of worms*
928 *viability using L-lactate assay*). A group of 12 worms were treated with the same volume of drug diluent

929 DMSO. This GWAS experiment was done twice independently. A total of 590 and 691 adult male worms
930 were collected, cultured *in vitro* and exposed to PZQ for the two experiments respectively.

931 Worm media supernatants (125 μ L) were collected in 96-well PCR plates after 24h in culture (to assess
932 the viability of the worms before PZQ treatment – adult male worms should release ≥ 40 nmol/h of lactate
933 in supernatant) and 48h post-treatment (to assess their viability after PZQ treatment). Plates containing
934 supernatant were immediately stored at -80 °C until processing. Lactate levels in supernatants were
935 quantified as described above (see *Metabolic assessment of worm viability using L-lactate assay*). We
936 phenotype the worms and categorize them into two groups: i) Recovered worms (i.e. releasing ≥ 40 nmol/h
937 of lactate in supernatant) and ii) Susceptible worms (i.e. releasing less 40 nmol/h of lactate in supernatant).
938 Among these two groups, we took the 20% of the treated worms releasing in their media the highest amount
939 of lactate (average L-lactate production \pm SD: Experiment 1 = 61.44 nmol/h \pm 13.16 / Experiment 2 = 56.38
940 nmol/h \pm 10.82) and the 20% of the treated worms releasing the lowest amount of lactate (average L-lactate
941 production \pm SD: Experiment 1 = 28.61 nmol/h \pm 5.32 / Experiment 2 = 23.04 nmol/h \pm 4.14), 48h post
942 PZQ treatment respectively.

943

944 DNA extraction and library preparation

945 We sequenced whole genomes of the two pools of recovered (i.e. resistant to PZQ, Experiment 1: 116
946 worms / Experiment 2: 137 worms) and susceptible worms (Experiment 1: 116 worms / Experiment 2: 137
947 worms). We then estimated allele frequencies in each pool to identify genome regions showing high
948 differentiation.

949 a. **gDNA extraction:** We extracted gDNA from pools of worms using the Blood and Tissue kit
950 (Qiagen). We homogenized worms in DNA extraction kit lysis buffer using sterile micro pestles.,
951 incubated homogenates (56 °C, 2 hour) and recovered gDNA in 200 μ L of elution buffer. We
952 quantified the worm gDNA recovered using the Qubit dsDNA HS Assay Kit (Invitrogen).

953 b. **Whole genome library preparation and sequencing:** We prepared whole genome libraries from
954 pools of worm gDNA in triplicate using the KAPA HyperPlus kit (KAPA Biosystems) according to

955 the manufacturer's protocol. For each library, we sheared 100 ng of gDNA by adaptive focused
956 acoustics (Duty factor: 10%; Peak Incident Power: 175; Cycles per Burst: 200; Duration: 180
957 seconds) in AFA tubes (Covaris S220 with SonoLab software version 7 (Covaris, Inc., USA)) to
958 recover fragmented DNA (150-200 bp). Library indexing was done using KAPA Dual Adapters at
959 15 μ M for 1h. We used 6 PCR cycles for post-ligation library amplification. We performed size
960 selection on the indexed-amplified libraries using KAPA Pure bead (0.7x first upper size cut; 0.9x
961 second lower size cut). We quantified libraries by qPCR using KAPA library quantification kit
962 (KAPA Biosystems) and their respective fragment size distribution was assessed by TapeStation
963 (Agilent). We sequenced the libraries on a HiSeq X sequencer (Illumina) using 150 bp pair-end
964 reads. Raw sequence data are available at the NCBI Sequence Read Archive (PRJNA699326).

965

966 Bioinformatic analysis

967 Jupyter notebook and scripts used for processing the sequencing data and identifying the QTL are available
968 on Github (https://github.com/fdchevalier/PZQ-R_DNA).

969 a. **Sequence analysis and variant calling:** We aligned the sequencing data against the *S. mansoni*
970 reference genome (schistosoma_mansoni.PRJEA36577.WBPS14) using BWA (v0.7.17) (67) and
971 SAMtools (v1.10) (68). We used GATK (v4.1.8.1) (69, 70) to mark PCR duplicates and recalibrate
972 base scores. We used the HaplotypeCaller module of GATK to call variants (SNP/indel) and the
973 GenotypeGVCFs module to perform a joint genotyping on each chromosome or unassembled
974 scaffolds. We merged VCF files using the MergeVcfs module. All these steps were automatized
975 using Snakemake (v5.14.0) (71).

976 b. **QTL identification:** We expect the genome region underlying resistance to be enriched in variants
977 from high lactate producing worms. To evaluate statistical evidence for such enrichment, we
978 examined the difference in allele frequencies between low and high lactate parasites across the
979 genome by calculating a Z-score at each bi-allelic site. To minimize bias, we weighed Z-scores by
980 including the number of worms in each treatment and the difference in the total read depth across

981 the triplicated libraries of each treatment at the given variant. We calculated Z-scores for each
982 biological replicate as follows:

$$983 \quad Z = \frac{p_1 - p_2}{\sqrt{p_0(1 - p_0) \left(\frac{1}{x \cdot n_1} + \frac{1}{x \cdot n_2} + \frac{1}{d_1} + \frac{1}{d_2} \right)}}$$

984 where p_1 and p_2 are the estimated allele frequencies in the low and high lactate parasites pools,
985 respectively; p_0 is the allele frequency under the null hypothesis $H_0: p_1 = p_2$ estimated from the average
986 of p_1 and p_2 ; n_1 and n_2 are the number of worms in the low and high lactate parasites pools,
987 respectively, factor x for each n reflecting the ploidy state ($x=2$); and d_1 and d_2 are the sequencing
988 depths for the low and high lactate parasite pools, respectively.

989

990 We combined Z-scores generated from each biological replicate as follows:

$$991 \quad Z_c = \frac{Z_1 + Z_2}{\sqrt{2}}$$

992 where Z_1 and Z_2 were Z-scores from replicate 1 and 2, respectively. The p-values were obtained by
993 comparing the negative absolute value of Z-scores to the standard normal distribution. To determine the
994 significant threshold, Bonferroni correction was calculated with $\alpha = 0.05$. These analyses are available
995 in the Jupyter notebook and associated scripts (https://github.com/fdchevalier/PZQ-R_DNA).

996

997 **Relationship between worm genotype at Chr 2 and 3 and PZQ-R phenotype**

998 To validate the impact of worm genotypes on its PZQ resistance phenotypes and determine whether PZQ-
999 R shows recessive, dominant or codominant inheritance, we determined the PZQ-R phenotype of individual
1000 worms, which were then genotyped for markers at the peak of the QTLs located.

1001

1002 *Measuring PZO-R in individual worms*

1003 We collected 120 SmLE-PZQ-R adult male worms, plated them individually in 96-well plates containing
1004 a mesh filter insert, cultured them *in vitro*, treated them with PZQ (24.3 µg/mL) and collected media
1005 supernatants before (after 24h in culture) and 48h post-treatment, and used L-lactate assays to determine
1006 PZQ-R status (see *Phenotypic selection*). We extracted gDNA from each worm individually. Briefly, we
1007 transferred worms into 96-well PCR plates, added 100 µL of 6% Chelex® solution containing 1%
1008 Proteinase K (20 mg/mL), incubated for 2h at 56 °C and 8 min at 100 °C, and transferred the supernatant
1009 containing worm gDNA into fresh labeled 96-well plates.

1010

1011 PCR-RFLP conditions for Chr.2 and Chr.3 loci

1012 We used PCR-RFLP to genotype single worms at loci marking QTL peaks on chr. 2 (C>A, chr SMV7_2:
1013 1072148) and chr. 3 (T>C, chr SMV7_3: 741987). Primers were designed using PerlPrimer v1.21.1 (75)
1014 (Table S4). We digested PCR amplicons for chr. 2 with BsiI (NEB) and chr. 3 with MseI (NEB), and
1015 visualized digested PCR amplicons by 2% agarose gel electrophoresis.

1016

1017 Quantitative PCR validation of copy number variation (CNV) in single worms

1018 We genotyped each individual worm for a deletion identified on chr. 3 at position 1220683- 1220861 bp
1019 using a custom quantitative PCR assay. This was done to examine the association between deletion of this
1020 genomic region and PZQ resistant genotype. We quantified the copy number in this region relative to a
1021 single copy gene from *S. mansoni* (α -tubulin 2, LeClech2019). The CNV genotype for each parasite
1022 corresponds to the ratio of the CNV copy number and the α -tubulin 2 gene copy number: 0=complete
1023 deletion, 0.5=one copy, 1=two copies. Methods and primers are described in Table S4. We then compared
1024 individual worm phenotypes for each of the three CNV genotypes (0, 1 or 2 copies) to determine the
1025 association between CNV and PZQ response.

1026

1027 **Marker assisted selection of resistant and susceptible parasite populations**

1028 Selection of SmLE-PZO-ER and SmLE-PZO-ES populations

1029 We separated the polymorphic SmLE-PZQ-R schistosome population based on chr. 3 QTL genotype using
1030 the PCR-RFLP as described. We exposed 960 inbred *B. glabrata* Bg121 snails to one miracidium SmLE-
1031 PZQ-R (66). At four weeks post-exposure, we identified infected snail ($N=272$), and collected cercariae
1032 from individual snails. We extracted cercarial DNA using 6% Chelex (66)), and genotyped each parasite
1033 for chr. 3 locus using our PCR-RFLP (Homozygous R/R: $n=89$ – 36%; Homozygous S/S: $n=39$ – 16%;
1034 Heterozygous R/S: $n=117$ – 49%) and determine their gender by PCR (72). We selected 32 R/R parasites
1035 (homozygous for the *Sm.TRPM_{PZQ}* resistant-associated allele) and 32 S/S genotypes (i.e. homozygous for
1036 the *Sm.TRPM_{PZQ}* sensitive-associated allele). For both R/R and S/S we used 13 males and 19 females. We
1037 exposed 5 hamsters to 800 cercariae of 32 R/R genotypes parasites and 5 hamsters to 800 cercariae 32 S/S
1038 genotyped parasites. This single generation marker assisted selection procedure generates two
1039 subpopulations: SmLE-PZQ-ER is expected to be enriched for parasites with R/R genotype and to show
1040 strong PZQ-R, while SmLE-PZQ-ES is enriched for S/S genotypes and is expected to be highly sensitive
1041 to PZQ).

1042

1043 PZQ IC_{50} with SmLE-PZQ-ER and SmLE-PZQ-ES

1044 Forty-five days after exposure to cercariae, we euthanized and perfused hamsters to recover adult
1045 schistosome worms for each of the two subpopulations (SmLE-PZQ-ER and SmLE-PZQ-ES). We
1046 separated worms by sex and we set adult males in 96-well plates containing 100 μ m mesh filter insert
1047 (Millipore) and cultured in 250 μ L DMEM complete media as described.

1048 We determined PZQ dose-response for both SmLE-PZQ-ER and SmLE-PZQ-ES population. We
1049 exposed individual worms ($N=60$ /population/treatment) to PZQ (0.1 μ g/mL, 0.3 μ g/mL, 0.9 μ g/mL, 2.7
1050 μ g/mL, 8.1 μ g/mL, 24.3 μ g/mL and 72.9 μ g/mL) or drug diluent (DMSO control). Worm media
1051 supernatants (125 μ L) were collected in 96-well PCR plates before treatment (after 24h in culture) and 48h
1052 post-treatment. We quantified lactate levels in supernatants described and we assess variation in lactate
1053 production for each individual worm.

1054

1055 *gDNA extraction and library preparation*

1056 SmLE-PZQ-ER and SmLE-PZQ-ES parasite populations were maintained in our laboratory. We recovered
1057 the F1 worms from each populations and extract gDNA from pools of adult males and females separately
1058 as described above. We prepared whole genome libraries from these pools in triplicate using the KAPA
1059 HyperPlus kit (KAPA Biosystems) as described (see *Whole genome library preparation and sequencing*).
1060 We sequenced the libraries on a HiSeq X sequencer (Illumina) using 150 bp paired-end reads. Sequence
1061 data are available at the NCBI Sequence Read Archive (accession numbers PRJNA701978).

1062

1063 *Bioinformatic analysis*

1064 The analysis was identical to the GWAS and QTL mapping analysis. This can be replicated with the Jupyter
1065 notebook and associated scripts (https://github.com/fdchevalier/PZQ-R_DNA).

1066

1067 **Transcriptomic analysis of resistant and susceptible schistosome worms to PZQ at juvenile (28 days)**
1068 **and adult (45 days) stages**

1069 *Sample collection*

1070 Juvenile and adult *S. mansoni* SmLE-PZQ-ER and SmLE-PZQ-ES worms were recovered by perfusion
1071 from hamsters at 28 days (juveniles) or 45 days (adults) post-infection. Worms from each population were
1072 placed in DMEM complete media, separated by sex, and aliquoted in sterile RNase free microtubes which
1073 were immediately snap-frozen in liquid nitrogen and stored at -80 °C until RNA extractions. For each
1074 subpopulation, (SmLE-PZQ-ER or SmLE-PZQ-ES), we collected 3 biological replicates of 30 males and 3
1075 replicates of 30 females for the 28d juvenile worms and 3 biological replicates of 30 males and 3 replicates
1076 of 60 females for the 45d adult worms.

1077

1078 *RNA extraction and RNAseq library preparation*

1079 ***a. RNA extraction***

1080 We extracted total RNA from all the *S. mansoni* adult and juvenile worms collected using the RNeasy Mini
1081 kit (Qiagen). Samples were randomized prior to RNA extraction to minimize batch effects. We
1082 homogenized worms in 600 μ L RNA lysis buffer (RTL buffer, Qiagen) using sterile micro pestles, followed
1083 by passing the worm lysate 10 times through a sterile needle (23 gauge). We recovered total RNA in 25 μ L
1084 elution buffer. We quantified the RNA recovered using the Qubit RNA Assay Kit (Invitrogen) and assessed
1085 the RNA integrity by TapeStation (Agilent - RNA integrity numbers of ~8.5–10 for all the samples).

1086 ***b. RNAseq library preparation***

1087 We prepared RNAseq libraries using the KAPA Stranded mRNA-seq kit (KAPA Biosystems) using 500ng
1088 RNA diluted in 50 μ L Tris-HCl (pH 8.0) for each library. We fragmented mRNA (6 min 94°C), indexed
1089 libraries using 3'-dTMP adapters (7 μ M, 1 hour at 20°C), and used 6 PCR cycles for post-ligation library
1090 amplification. We quantified indexed libraries by qPCR (KAPA library quantification kit (KAPA
1091 Biosystems)) and assessed their fragment size distribution by TapeStation (Agilent). We sequenced the
1092 libraries on a HiSeq 4000 sequencer (Illumina) using 150 bp pair-end reads, pooling 12 RNAseq
1093 libraries/lane. Raw sequence data are available at the NCBI Sequence Read Archive under accession
1094 numbers PRJNA704646.

1095 ***c. Bioinformatic analysis.***

1096 To identify differentially expressed genes between the different groups, we aligned the sequencing data
1097 against the *S. mansoni* reference genome (schistosoma_mansoni.PRJEA36577.WBPS14) using STAR
1098 (v2.7.3a) (ref). We quantified gene and isoform abundances by computing transcripts per million values
1099 using RSEM (v1.3.3) (ref). We compared these abundances between groups (ES/ER, males/females,
1100 juveniles/adults) using the R package EBSeq (v1.24.0) (ref). Jupyter notebooks and associated scripts are
1101 available on Github (https://github.com/fdchevalier/PZQ-R_RNA).

1102

1103 **Manipulation of *Sm.TRPM_{PZO}* channel expression or function:**

1104 *RNA interference*

1105 We used RNA interference to knock down the expression of Smp_246790 gene in order to functionally
1106 validate the implication of *Sm.TRPM_{PZQ}* on schistosome PZQ resistance. SmLE-PZQ-R adult male worms
1107 were freshly recovered from infected hamsters and placed in 24-well plates for in vitro culture (10 adult
1108 male worms/well).

1109 ***a. siRNA treatment on S. mansoni adult male worms***

1110 Small inhibitory RNAs (siRNAs) targeting specific schistosome genes were designed using the on-line IDT
1111 RNAi Design Tool (<https://www.idtdna.com/Scitools/Applications/RNAi/RNAi.aspx>) (Table S2) and
1112 synthesized commercially by Integrated DNA Technologies (IDT, Coralville, IA). To deliver the siRNAs,
1113 we electroporated schistosome parasites (10 adults/group – each group done in triplicate) in 100 μ L RPMI
1114 medium containing 2.5 μ g siRNA or the equivalent volume of ddH₂O (no siRNA control), in a 4 mm cuvette
1115 by applying a square wave with a single 20 ms impulse, at 125 V and at room temperature (Gene Pulser
1116 Xcell Total System (BioRad)) (76, 77). Parasites were then transferred to 1 mL of complete DMEM media
1117 in 24-well plates. After overnight culture, medium was replaced with fresh DMEM complete media. We
1118 measured gene expression by quantitative real-time PCR (RT-qPCR) 2 days after siRNA treatment.

1119 ***b. dsRNA treatment on S. mansoni adult male worms***

1120 We synthesized double-stranded RNA according to Wang et al., 2020 (Table S2). For dsRNA treatment, 10
1121 adult male worms/group (each group done in triplicate) were cultured in 1 mL DMEM complete media and
1122 treated with 90 μ g dsRNA at day 0, day 1 and day 2. Media was changed every 24h and fresh dsRNA was
1123 added. On day 3, we harvested worms and measured gene expression by quantitative real-time PCR (RT-
1124 qPCR).

1125 ***c. RNA extraction and gene expression analysis by RT-qPCR***

1126 We extracted total RNA from parasites ($N=10$ worms/sample) using the RNeasy Mini kit (Qiagen) (see
1127 *RNA extraction*). Complementary DNA (cDNA) was generated from extracted RNA (500 ng - 1 μ g) using
1128 SuperScript-III and Oligo-dT primers (ThermoFisher). Relative quantification of genes of interest was
1129 performed in duplicate by qPCR analysis using QuantStudio 5 System (Applied Biosystems) and SYBR
1130 Green master mix (ThermoFisher), compared with a serially diluted standard of PCR products (generated

1131 from cDNA) for each of the gene tested (66). Standard curves allow evaluating the efficiency of each pairs
1132 of primers, for both housekeeping and target genes using QuantStudio Design and Analysis Software.
1133 Expression was normalized to SmGAPDH housekeeping gene (Table S2) using the efficiency $E^{\Delta\Delta Ct}$ method
1134 (78).

1135

1136 *Specific Sm.TRPM_{PZQ} chemical inhibitor and activators*

1137 We used specific chemical inhibitor and activators (Chulkov *et al.*, in prep) to manipulate the function of
1138 Sm.TRPM_{PZQ} to examine the impact on PZQ-response. We placed individual SMLE-PZQ-ER and SMLE-
1139 PZQ-ES adult male worms in 96-well plates with 100 μ m mesh filter insert containing DMEM complete
1140 media and cultured described above (see *Metabolic assessment of worm viability using L-lactate assay*).
1141 After 24h in culture, 20 worms from each population were treated either with a cocktail combining PZQ (1
1142 μ g/mL) and i) 50 μ M of *Sm.TRPM_{PZQ}* blocker (MB2) or ii) 10 μ M, 25 μ M or 50 μ M of *Sm.TRPM_{PZQ}*
1143 activator (MV1) respectively or iii) drug diluent (DMSO). We also set up control plates to evaluate the
1144 impact of *Sm.TRPM_{PZQ}* blocker or activator alone. In that case, 20 worms from each population were treated
1145 with a cocktail combining drug diluent DMSO and *Sm.TRPM_{PZQ}* blocker (MB2) or activator (MV1) at the
1146 same concentrations mentioned above. Worms were exposed to these drug cocktails for 24h, washed 3
1147 times with drug-free medium, and incubated (37°C, 5% CO₂) for 2 days.

1148 We collected Worm media supernatants (125 μ L) in 96-well PCR plates before treatment (after 24h
1149 in culture) and 48h post-treatment and Lactate levels in supernatants were quantified as described above
1150 (see *Metabolic assessment of worm viability using L-lactate assay*). We used these results to determine the
1151 impact of blockers or activators on variation in lactate production.

1152

1153 *In vivo parasite survival after PZQ treatment*

1154 We used 24 female Balb/C mice (purchased from Envigo at 6 weeks-old and housed in our facility for one
1155 week before use) split into two groups: one group exposed by tail immersion to SmLE-PZQ-ER (80
1156 cercariae/mouse from 40 infected snails) and the second one to SmLE-PZQ-ES (80 cercariae/mouse from

1157 40 infected snails). Each mouse was identified by a unique tattoo ID and an ear punch for assessing
1158 treatment status (PZQ or drug diluent control). Immediately after infection, we stained the content of each
1159 infection vial with 10 μ L 0.4% Trypan blue and counted all the cercarial tails/heads or complete cercariae
1160 to determine the cercarial penetration rate for each mouse. We kept infected mice in 4 cages (2
1161 cages/parasite populations and 6 animals per cage) at 21-22° C and 39%–50% humidity and monitored them
1162 daily.

1163 Forty days post-infection, we weighed mice and treated them by oral gavage with either 120mg/kg
1164 of PZQ (diluted in 1% DMSO + vegetable oil – Total volume given/mouse: 150 μ L) or the same volume
1165 of drug diluent only (control group). To minimize batch effects, 3 mice were treated with PZQ and 3 with
1166 the drug diluent per cage for each parasite group (SmLE-PZQ-ER or SmLE-PZQ-ES). Mice were monitored
1167 daily until euthanasia and perfusion (65), at day 50 post-infection. We recorded the weight of each mouse
1168 before euthanasia. After euthanasia and perfusion, we also weighted the liver and spleen of each individual.
1169 We carefully recovered worms from the portal vein, liver and intestine mesenteric venules of each mouse.
1170 Worms were separated by sex and counted.

1171

1172 **Sm.TRPM_{PZQ} variants in *S. mansoni* field samples**

1173 Variants identification in exome-sequenced data from natural *S. mansoni* parasites

1174 We utilized exome sequence data from *S. mansoni* from Africa, South America and the middle East to
1175 investigate variation in *Sm.TRPM_{PZQ}*. African miracidia were from the Schistosomiasis collection at the
1176 Natural History Museum (SCAN) (73), Brazilian miracidia and Omani cercariae and adult worms were
1177 collected previously. We have previously described methods and generation of exome sequence from *S.*
1178 *mansoni* samples (51, 52). Data were analyzed the same way as described in Chevalier et al. (52). Code is
1179 available in Jupyter notebook and scripts associated (https://github.com/fdchevalier/PZQ-R_field).

1180

1181 Sanger re-sequencing to confirm the presence of the *Sm.TRPM_{PZQ}* field variants

1182 To confirm the presence of the variants in *Sm.TRPM_{PZQ}* gene from our exome-sequenced natural *S. mansoni*
1183 parasites (when read depth was <10 reads), we performed Sanger re-sequencing of eight *Sm.TRPM_{PZQ}* exons
1184 (i.e. exon 3, 4, 23, 25, 27, 29 and 34) where either nonsense mutations (leading to truncated protein) or non-
1185 synonymous mutation located close to the PZQ binding site (21) were identified. Primers and conditions
1186 are listed in Table S4.

1187

1188 Sanger sequencing analysis

1189 We scored variants using PolyPhred software (v6.18) (Nickerson et al., 1997) which relies on Phred
1190 (v0.020425.c), Phrap (v0.990319), and Consed (v29.0) software, analyzing each exon independently. We
1191 identified single nucleotide polymorphisms using a minimum phred quality score (-q) of 25, a minimum
1192 genotype score (-score) of 70, and a reference sequence of the *Sm.TRPM_{PZQ}* gene from the chromosome 3
1193 of *S. mansoni* reference genome (schistosoma_mansoni.PRJEA36577.WBPS14). Variant sites were labeled
1194 as non-reference alleles if they differed from the reference sequence. We identified insertion/deletion
1195 (indel) polymorphisms using a minimum phred quality score (-q) of 25, a minimum genotype score (-score)
1196 of 70. Polymorphisms were visually validated using Consed. All the sequences were submitted to GenBank
1197 (GenBank accession no KU951903-KU952091). These analyses are available in the Jupyter notebook and
1198 associated scripts (https://github.com/fdchevalier/PZQ-R_DNA).

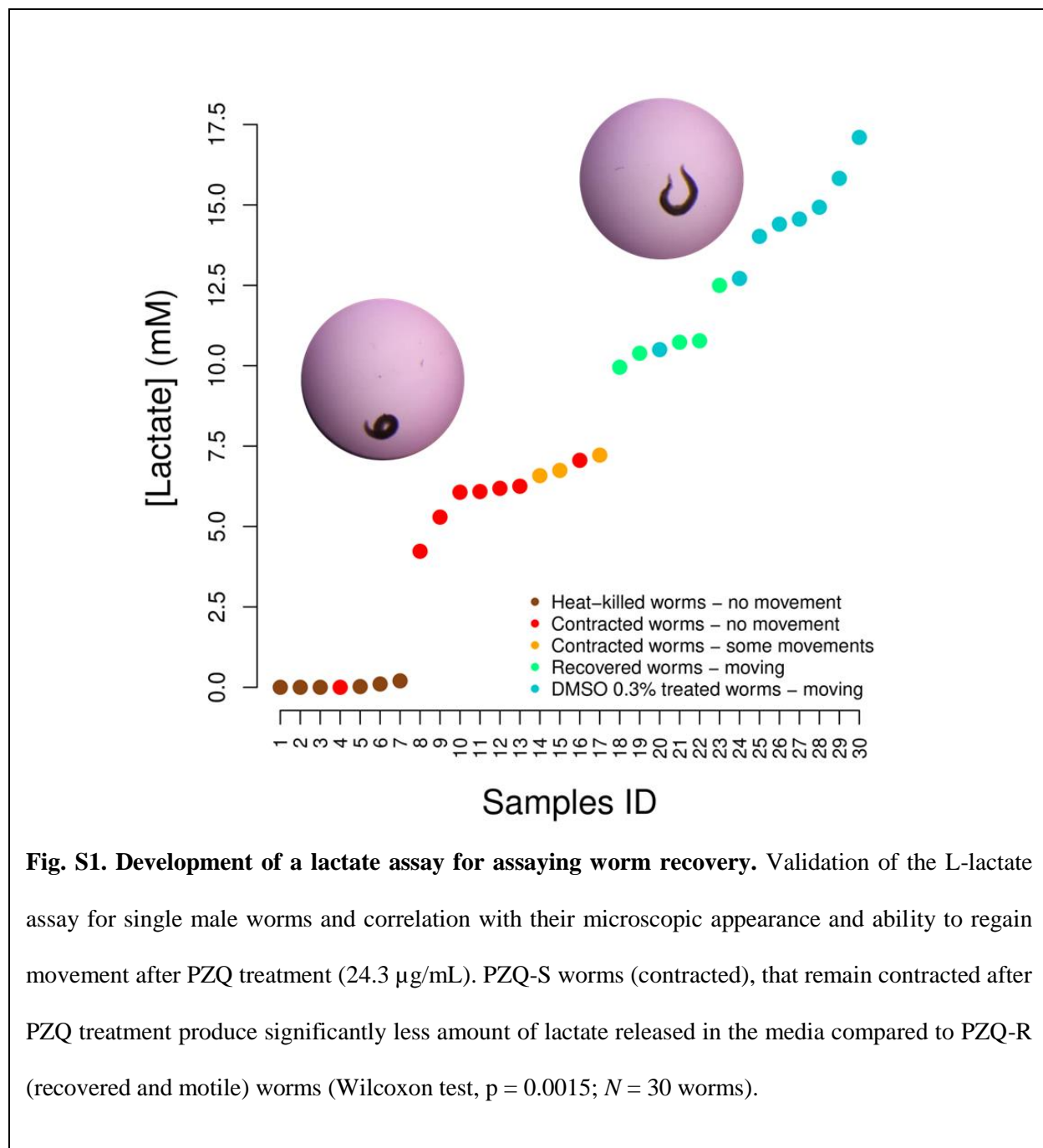
1199

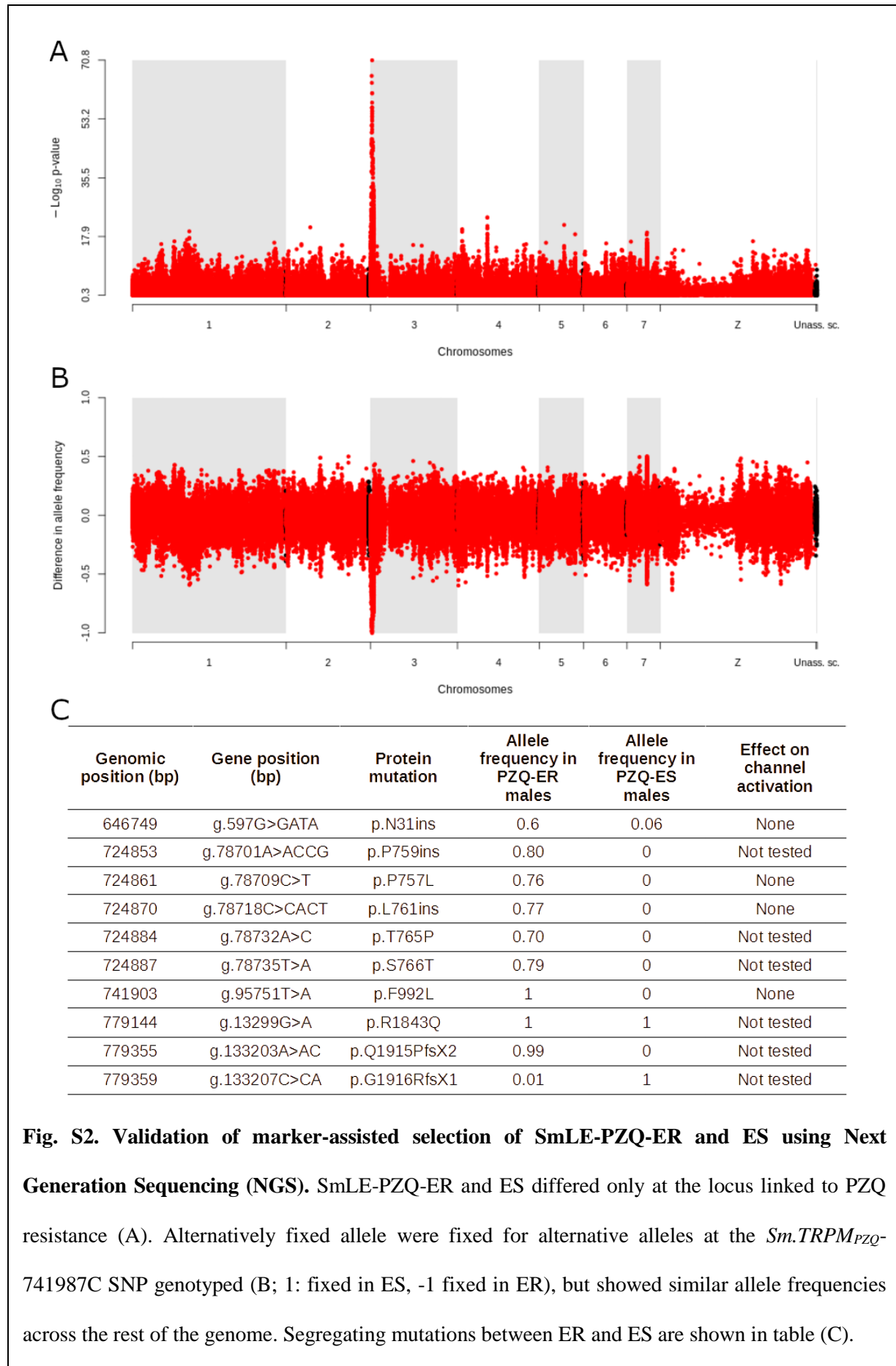
1200 Statistical analysis

1201 All statistical analyzes and graphs were performed using R software (v3.5.1) (74). We used the drc package
1202 from R to analyze all our dose-response datasets using a four-parameter log-logistic function to fit curves.
1203 We used the Readqpcr and Normqpcr packages to analyze all our RT-qPCR datasets, using the $efficiency^{\Delta\Delta Ct}$
1204 method. When data were not normally distributed (Shapiro test, $p < 0.05$), we compared results with non-
1205 parametric tests: Chi-square test, Kruskal-Wallis test followed by pairwise Wilcoxon-Mann-Whitney post-
1206 hoc test or a simple pairwise comparison Wilcoxon-Mann-Whitney test. When data followed a normal

1207 distribution, we used one-way ANOVA or a pairwise comparison Welch *t*-test. The confidence interval of
1208 significance was set to 95% and *p*-values less than 0.05 were considered significant.

1209 SUPPLEMENTARY FIGURES





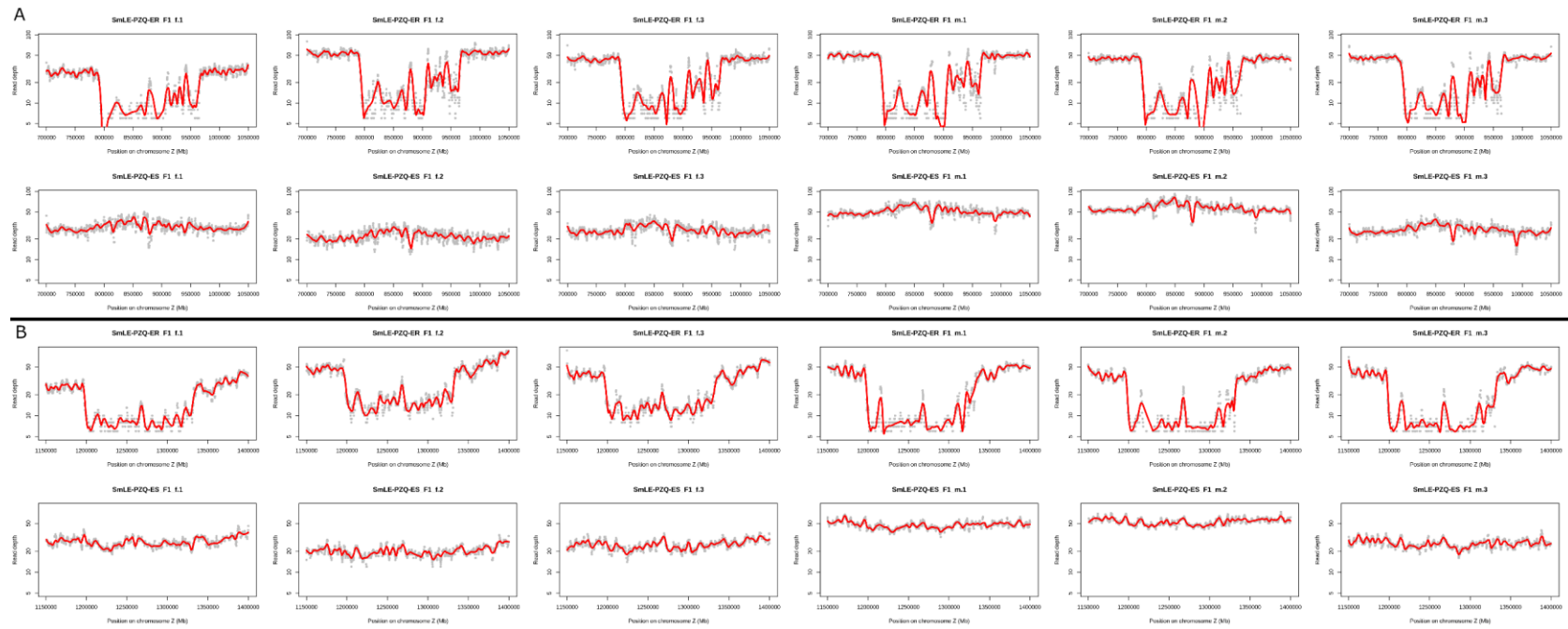


Fig. S3. Large deletions adjacent to *Sm.TRPM_{PZQ}* and *SOX13* transcription factor. Sequencing of adult parasites recovered from SmLE-PZQ-ER and SmLE-PZQ-ES populations also revealed that the 100 kb (A) and the 150 kb (B) deletions were close to fixation in the SmLE-PZQ-ER population. The first row of each panel refers to the ER population, the second to the ES population. The first three columns refer to the female, the last three columns to the males.

1212

1213

1214

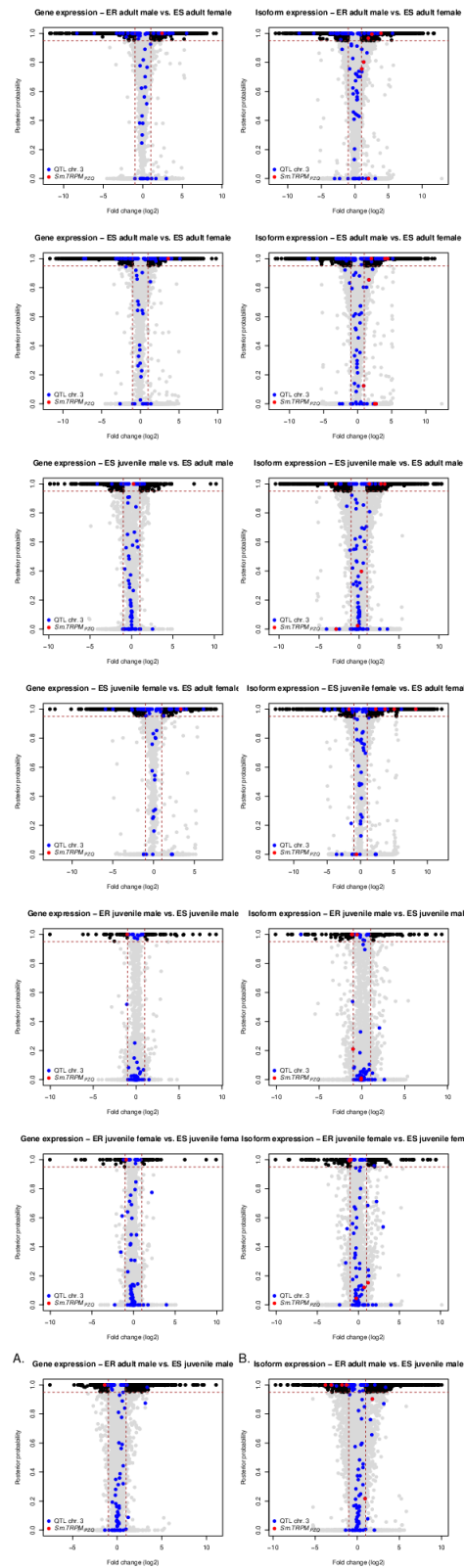
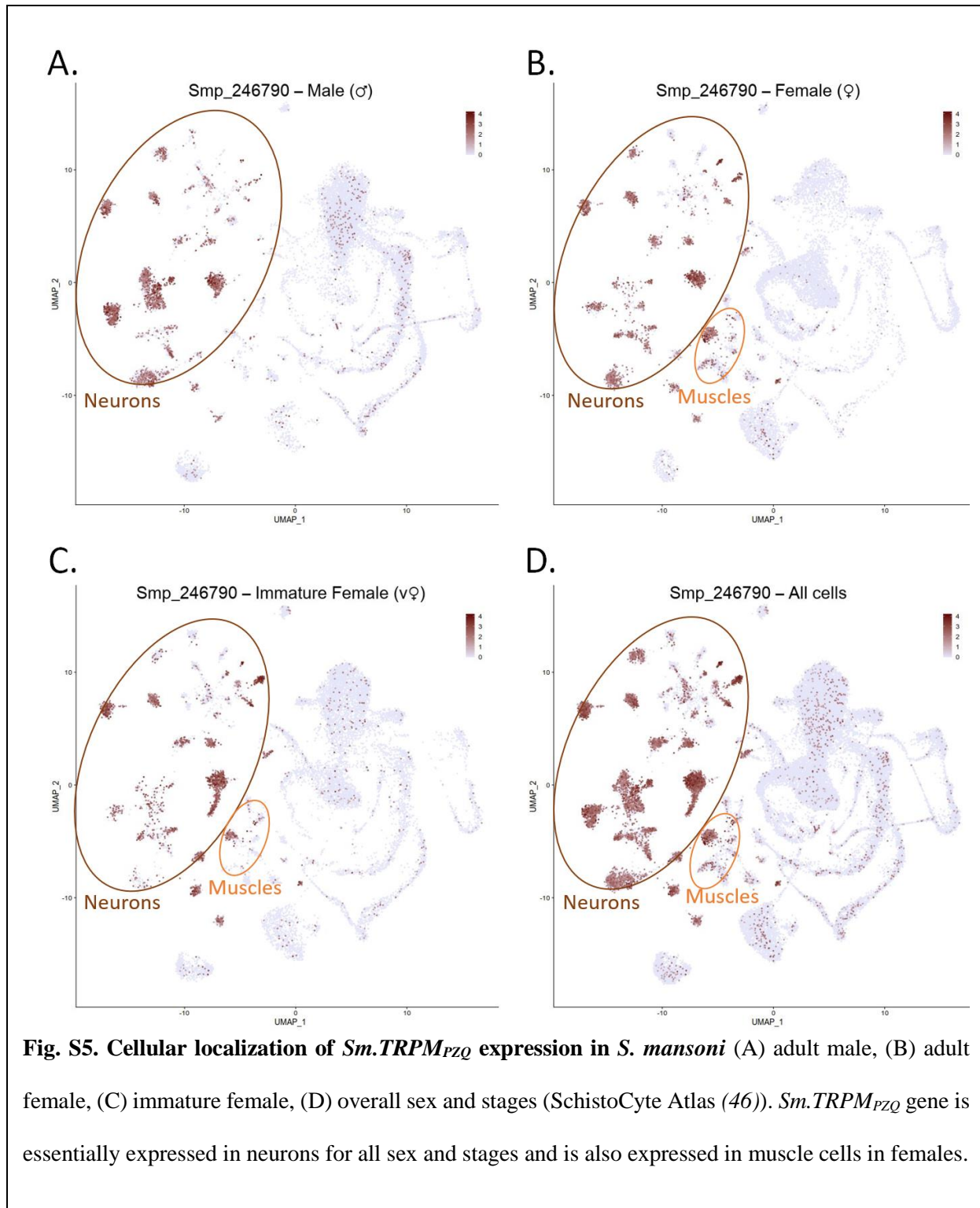


Fig. S4. Detailed genes and isoforms expression in SmLE-PZQ-ER and SmLE-PZQ-ES parasites. Comparison of genes and isoforms expression between SmLE-PZQ-ER and ES parasites for each sex (i.e. male and female) and each parasite stage (i.e. adult worm and juvenile worm)



1216

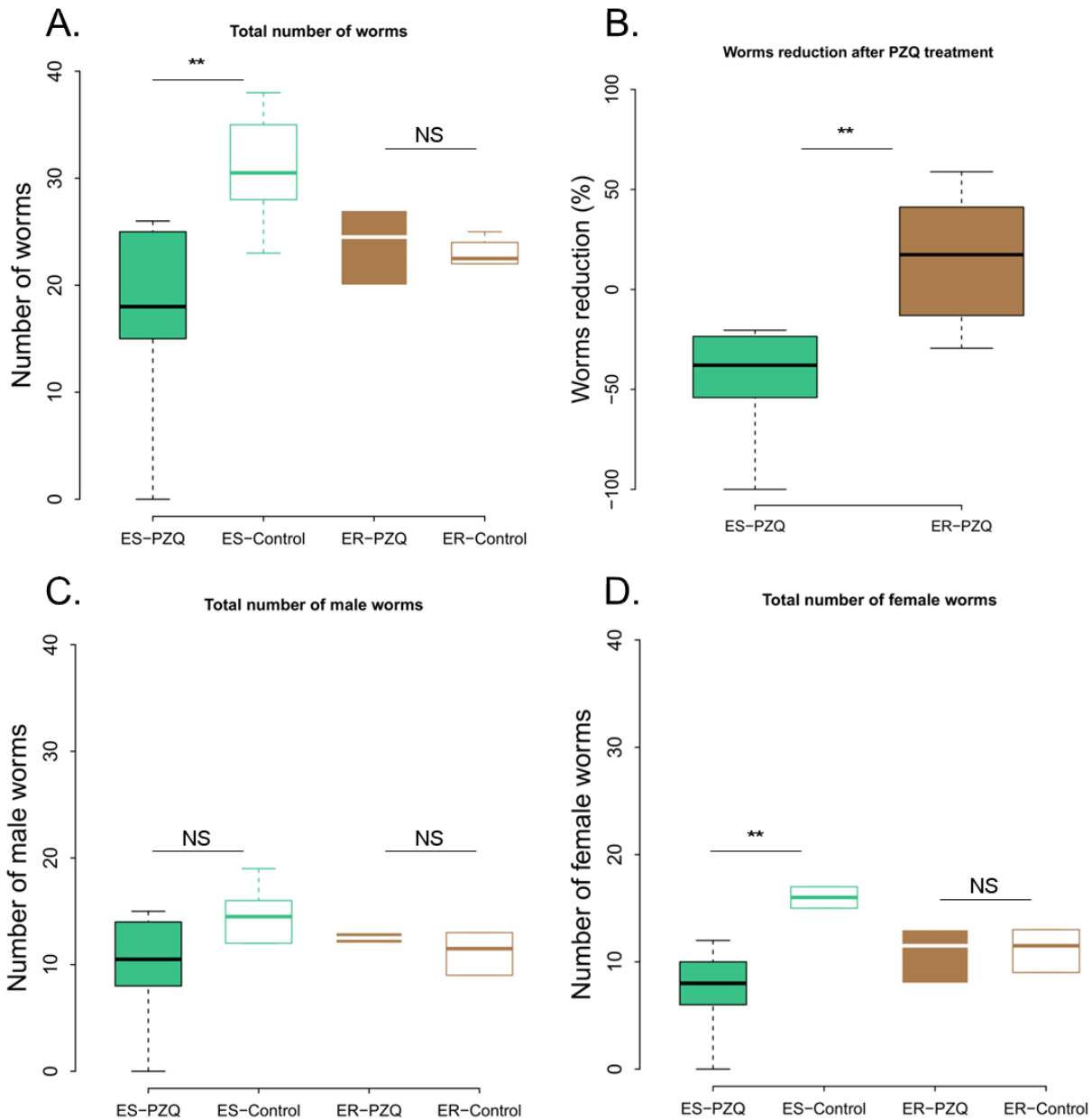
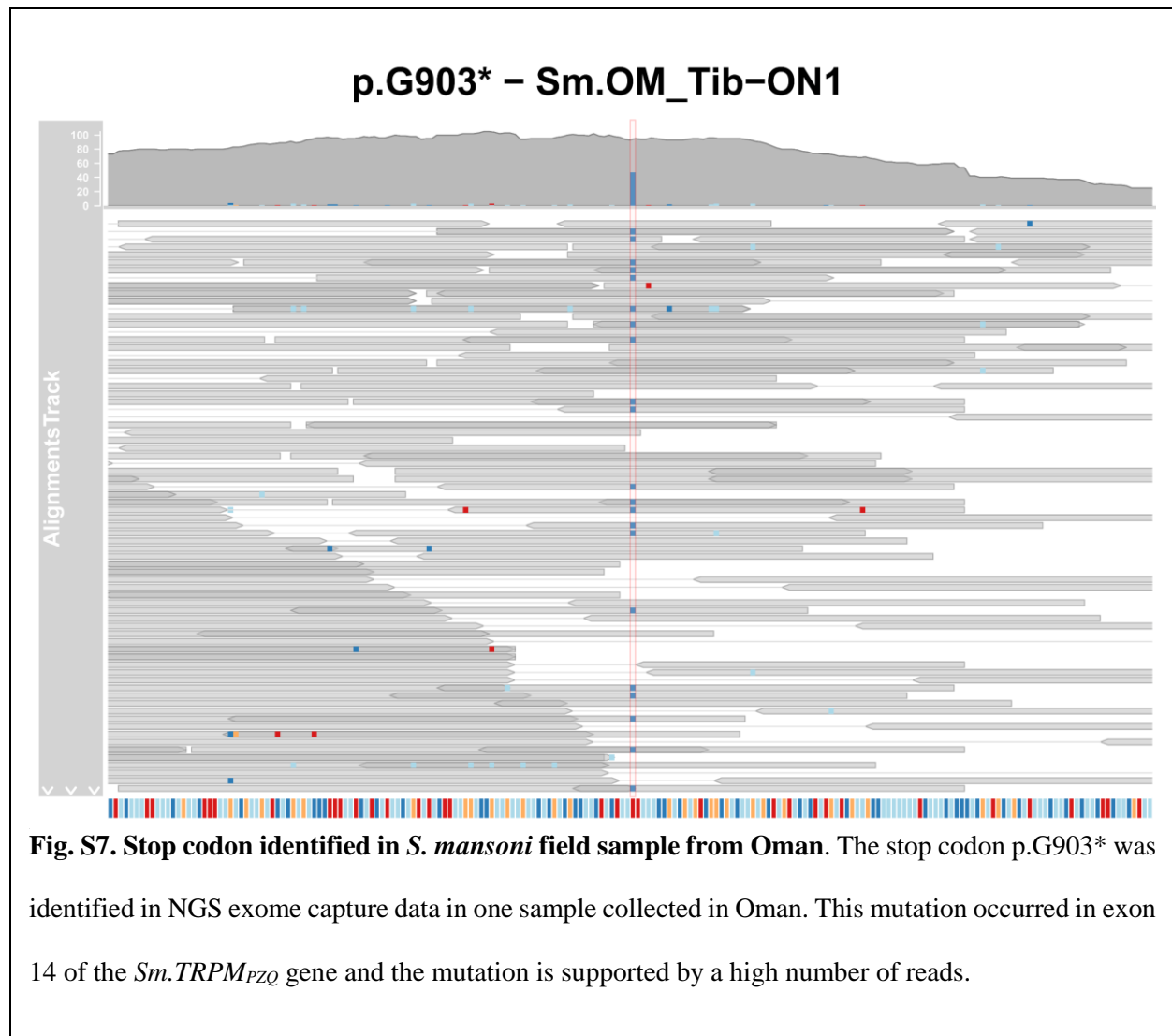


Fig. S6. Impact of *in vivo* PZQ treatment on SmLE-PZQ-ER and SmLE-PZQ-ES parasites. Balb/c mice were infected with either SmLE-PZQ-ER or SmLE-PZQ-ES parasite populations and treated with 120 mg/kg of PZQ or DMSO (control group). (A). We observed no significant reduction in worm burden in SmLE-PZQ-ER parasites when comparing PZQ-treated and control (DMSO) treated animals (Wilcoxon test, $p = 0.393$). In contrast, we recovered significantly lower numbers of worms from PZQ-treated versus untreated mice infected with the SmLE-PZQ-ES parasite population (Wilcoxon test, $p = 0.008$). (B). The percent reduction observed was significantly different between the SmLE-PZQ-ES and SmLE-PZQ-ER parasites (Wilcoxon test, $p = 0.0129$). (C). While interestingly, we did not reach significance for male worms (Wilcoxon test, $p = 0.089$), (D). we observed a large reduction in numbers of female worms recovered from PZQ-treated SmLE-PZQ-ES parasites relative to untreated animals (Wilcoxon test, $p = 0.008$) ($N = 24$ mice – 6 mice/group; NS: No significant difference between groups; * $p < 0.05$; ** $p \leq 0.02$; *** $p \leq 0.002$).



1218 **Table S1. Genes in QTL regions on chr 2 and 3.**

1219 *Separate file*

1220 **Table S2. Summary table of RNAi for Sm.TRPM_{PZQ}.** siRNA sequences and primers used to generate dsRNA. Primer sequences used for RT-
 1221 qPCR to quantify gene expression after RNAi treatment on worms (Chr.: Chromosome; E: Exon). * siRNA negative (scramble siRNA) and positive
 1222 control (SmAP) have been used from Krautz-Peterson *et al.* (79).

Location on the genome	Genomic coordinates	Type	Sequence (5'-3' orientation)	Expected size (bp)	Usage
Chr. 3	646335-646359	siRNA SmTRP #1 (isoform 5) E1-E2	AGUACUUUGUUGAAGUCCUUGAATA	-	siRNA
Chr. 3	724927-724951	siRNA SmTRP #2 (isoform 5) E10-E20	CAGCAUUUUUAGAAUGUGAUAAATA	-	siRNA
Chr. 3	767394-767415	siRNA SmTRP #3 (isoform 6) E23-E32	ACCAAGGAGAAUAUGACAUUGAATT	-	siRNA
Chr. 4	33713410-33713434	siRNA SmAP* (positive control)	CCACAAGCAUGUUCUCUJACAUACA	-	siRNA
-	-	Scrambled siRNA* (negative control)	CUUCCUCUCUUUCUCUCCCUUGUGA	-	siRNA
Chr. 3	646449-646472	dsRNA SmTRP #1 (isoform 1-5) – Forward primer	GAAACTGGTACTTTATCCAAGTCC	614	dsRNA generation
Chr. 3	685256-685276	dsRNA SmTRP #1 (isoform 1-5) – Reverse primer	TCAGCTGCTTTCCATAAACCT		dsRNA generation
Chr. 3	700008-700029	dsRNA SmTRP #2 (isoform 6) – Forward primer	TACAAGTCAACAAAGTGGACCT	602	dsRNA generation
Chr. 3	706699-706721	dsRNA SmTRP #2 (isoform 6) – Reverse primer	CTTCAATGATGGATTCAAGCCTG		dsRNA generation
-	-	EGFP Forward primer with T7 promoter (negative control)	GGTAATACGACTCACTATAGGGAGGTAAACGGCCACAA GTTCAG	591	Control RNAi (dsRNA)
-	-	EGFP Reverse primer with T7 promoter (negative control)	GGTAATACGACTCACTATAGGGAGGTGCTCAGGTAGTG GTTGTC		Control RNAi (dsRNA)
Chr. 3	756865-756887	SmTRP _{qF1} – Forward primer	AGTCCTACTTCTGAACAACAAGG	124	RT-qPCR
Chr. 3	757787-757808	SmTRP _{qR1} – Reverse primer	TATATTCCACGGTTCTAGCCTG		RT-qPCR

Chr. 3	787906-787927	SmTRP_qF2 pyrophosphatase domain (isoform 6) – Forward primer	ATCAGCAGTTTGATTACACGTC	199	RT-qPCR
Chr. 3	791384-791407	SmTRP_qR2 pyrophosphatase domain (isoform 6) – Reverse primer	GAAGTTGAGCTCCTTTACTTTTCAG		RT-qPCR
Chr. 4	3371912 4- 3371914 7	SmAP_qF1 – Forward primer	TCAACTCAGATAGACTCACAACAG	76	RT-qPCR
Chr. 4	3372031 8- 3372033 8	SmAP_qR1 – Reverse primer	TTAAATGGCCCTTTACACCT		RT-qPCR
Chr. 1	4316475 5- 4316477 1	SmGAPDH_qF2 - Forward primer	CATTGATAAAGCTCAGGCTCAT	195	RT-qPCR
Chr. 1	4316453 9- 4316456 2	SmGAPDH_qR2 - Reverse primer	AACTTATCATGAATGACCTTAGCC		RT-qPCR

1224 **Table S3. Mutations present in *Sm.TRPM_{PZQ}* in natural schistosome populations from 3 African**
1225 **countries (Senegal, Niger, Tanzania), the Middle East (Oman) and South America (Brazil).**
1226 *Separate file*

1227 **Table S4. Summary table of all the primer sequences** used for i) PCR-RFLP and CNV quantification for single worm genotyping, ii) Sanger
 1228 sequencing of Sm.TRPM_{PZQ} in field collected *S. mansoni* parasites (Chr. : Chromosome; E: Exon).

Location on the genome	Genomic coordinates	Exon coordinate (Gene exon number)	Type	Sequence (5'-3' orientation)	Expected size (bp)	Usage
Chr. 2	1071798-1071820	-	Chr. 2 PCR-RFLP – Forward primer	GACAAGAACCCATCAAGTAACAT	618	PCR-RFLP genotyping ^a
Chr. 2	1072394-1072415	-	Chr. 2 PCR-RFLP – Reverse primer	GACAAAGCTACCACAACAACT		PCR-RFLP genotyping ^a
Chr. 3	741747-741766	-	Chr. 3 PCR-RFLP – Forward primer	TCGTAATAAACATGGTCGTC	421	PCR-RFLP genotyping ^a
Chr. 3	742148-742167	-	Chr. 3 PCR-RFLP – Reverse primer	TCGACTACAGAATGATGTAA		PCR-RFLP genotyping ^a
Chr. 3	1220683-1220701	-	Chr. 3 CNV genotyping – Forward primer	GAAACATTCTGGTCCACCC	179	CNV genotyping (qPCR) ^b
Chr. 3	1220840-1220861	-	Chr. 3 CNV genotyping – Reverse primer	TGGCTTCAGTATTGAAAGTTGC		CNV genotyping (qPCR) ^b
Chr. 4	46055234-46055257	-	Chr. 4 α -tubulin 2 – Forward primer	CGACTTAGAACCAAATGTTGTAGA	190	qPCR (CNV relative quantification) ^b
Chr. 4	46055405-46055424	-	Chr. 4 α -tubulin 2 – Reverse primer	GTCCACTACATTGATCCGCT		qPCR (CNV relative quantification) ^b
Chr. 3	693769-693788	693738-693904 (4)	Sm.TRPM _{PZQ} E 3 – Sanger sequencing – Forward primer	AGGAGTAATGAAGCTAACTG	140	Sanger sequencing ^c
Chr. 3	693891-693909	693738-693904 (4)	Sm.TRPM _{PZQ} E 3 – Sanger sequencing – Reverse primer	GTTACCTCATGTAAAGCTG		Sanger sequencing ^c
Chr. 3	699775-699792	699733-700482 (5)	Sm.TRPM _{PZQ} E 4 – Sanger sequencing – Forward primer	GCTGAAGATAGTGAACCA	271	Sanger sequencing ^c
Chr. 3	700027-700046	699733-700482 (5)	Sm.TRPM _{PZQ} E 4 – Sanger sequencing – Reverse primer	TGTGTTGTAGAACTGATAGG		Sanger sequencing ^c
Chr. 3	764334-764354	764295-764594 (27)	Sm.TRPM _{PZQ} E 23 – Sanger sequencing – Forward primer	GATGGATGGAATAAATTAGAT	288	Sanger sequencing ^c
Chr. 3	764603-764622	764295-764594 (27)	Sm.TRPM _{PZQ} E 23 – Sanger sequencing – Reverse primer	CAACATAGAAACAAATCAAA		Sanger sequencing ^c

Chr. 3	771992-772011	772107-772214 (29)	Sm.TRPM _{PZQ} E 25 – Sanger sequencing – Forward primer	ATAATGCTTGATTCCCTTCC	345	Sanger sequencing ^c
Chr. 3	772318-772337	772107-772214 (29)	Sm.TRPM _{PZQ} E 25 – Sanger sequencing – Reverse primer	TAATCCCACATAGATGACAG		Sanger sequencing ^c
Chr. 3	774815-774832	774968-775167 (31)	Sm.TRPM _{PZQ} E 27 – Sanger sequencing – Forward primer (1)	CTCCATCAGGAGAAACAG	418	Sanger sequencing ^c
Chr. 3	775214-775233	774968-775167 (31)	Sm.TRPM _{PZQ} E 27 – Sanger sequencing – Reverse primer (1)	AAGTATCGTGGCTTATTAGG		Sanger sequencing ^c
Chr. 3	774815-774832	774968-775167 (31)	Sm.TRPM _{PZQ} E 27 – Sanger sequencing – Forward primer (2)	CTCCATCAGGAGAAACAG	459	Sanger sequencing ^c
Chr. 3	775255-775274	774968-775167 (31)	Sm.TRPM _{PZQ} E 27 – Sanger sequencing – Reverse primer (2)	GTACACTTAATTCGTACGAC		Sanger sequencing ^c
Chr. 3	778437-778454	778446-778595 (33)	Sm.TRPM _{PZQ} E 29 – Sanger sequencing – Forward primer	ATGACTCAGGGTATTGGA	287	Sanger sequencing ^c
Chr. 3	778706-778724	778446-778595 (33)	Sm.TRPM _{PZQ} E 29 – Sanger sequencing – Reverse primer	GGGTTGATGGATATTTGGG		Sanger sequencing ^c
Chr. 3	787904-787924	787852-788001 (38)	Sm.TRPM _{PZQ} E 34 – Sanger sequencing – Forward primer	TTATCAGCAGTTTGATTACAC	116	Sanger sequencing ^c
Chr. 3	788001-788020	787852-788001 (38)	Sm.TRPM _{PZQ} E 34 – Sanger sequencing – Reverse primer	CATTATGTTCTATCCATACC		Sanger sequencing ^c

1229

1230

1231 ^a PCR conditions for RFLP genotyping: reactions contained 9.325 µL sterile water, 1.5 µL 10x buffer, 1.2 µL dNTP (2.5 mM each), 0.9 µL MgCl₂,

1232 0.5µL each primer (10 µM), 0.075 µL *Taq* polymerase (TaKaRa) and 1µL of gDNA template using the following program: 95 °C for 5 minutes, [95

1233 °C for 30s, 55 °C for 30s, and 72 °C for 1min] × 35 cycles, 72 °C for 10 minutes.

1234

1235 ^bqPCR genotyping methods: we conducted qPCR in duplicate for each reaction (samples and standards). Reactions consisted of 5 μ L SYBR Green
1236 PCR master mix (Applied Biosystems), 3.4 μ L sterile water, 0.3 μ L of each primer and 1 μ L of standard PCR product or sample gDNA. We used
1237 the following program: 95 °C for 10 minutes, [95 °C for 15s and 60 °C for 1 minute] \times 40 cycles followed by a melting curve step (15s at 95 °C and
1238 then rising in 0.075 °C increments/second from 60 °C to 95 °C), to check for the uniqueness of the product amplified. We plotted standard curves
1239 using seven 10-fold dilutions of a purified i) α -tubulin 2 PCR product (α -tubulin 2 copies. μ L⁻¹: $2.21 \times 10^2 - 2.21 \times 10^7$, efficiency= 87.56%) and ii)
1240 CNV region PCR product (Sm.CNV region copies. μ L⁻¹: $8.40 \times 10^1 - 8.40 \times 10^6$, efficiency= 86.17%). PCR products for standard curves were
1241 generated as described in LeClech *et al.* (80). The number of CNV region and α -tubulin 2 copies in each sample was estimated according to the
1242 standard curve (QuantStudio Design and Analysis Software). All the primers were designed using PerlPrimer v1.21.1 (75).

1243

1244 ^cPCR conditions for Sanger sequencing: PCRs were performed using the TaKaRa Taq kit (Clontech, USA). For Exon 25 and 27, PCR reactions
1245 contained 8.325 μ L sterile water, 1.5 μ L 10X buffer, 1.2 μ L dNTP (2.5 mM each), 0.9 μ L MgCl₂ (25 mM), 0.5 μ L each primer (10 μ M), 0.075 μ L
1246 Taq polymerase (5 U/ μ L) and 2 μ L of DNA template (WGA DNA from *S. mansoni* field collected miracidia from infected patients) (Total reaction
1247 volume: 15 μ L). For Exon 3, 4, 12, 23, 29 and 34, PCR reactions were done in a total volume of 50 μ L (keeping similar volume ratio between the
1248 reagents) with 2 μ L of DNA template. We used a SimpliAmp Thermal cycler (Applied Biosystems) with the following program: 95 °C for 5 min;
1249 95 °C for 30 s, 53 °C for 45 s, 72 °C for 45 s, for 35 cycles; then 72 °C for 10 min. We verified the presence and size of all PCR products on 2%
1250 agarose gels. Ten microliters of PCR products were then cleaned up by adding 4 μ L of ExoSAP-IT (Affymetrix USB products) and 2 μ L of sterile
1251 water and Sanger sequenced in both directions.